iScience

CellPress
OPEN ACCESS

Article

Frequency dominates intensity of future heat waves over India

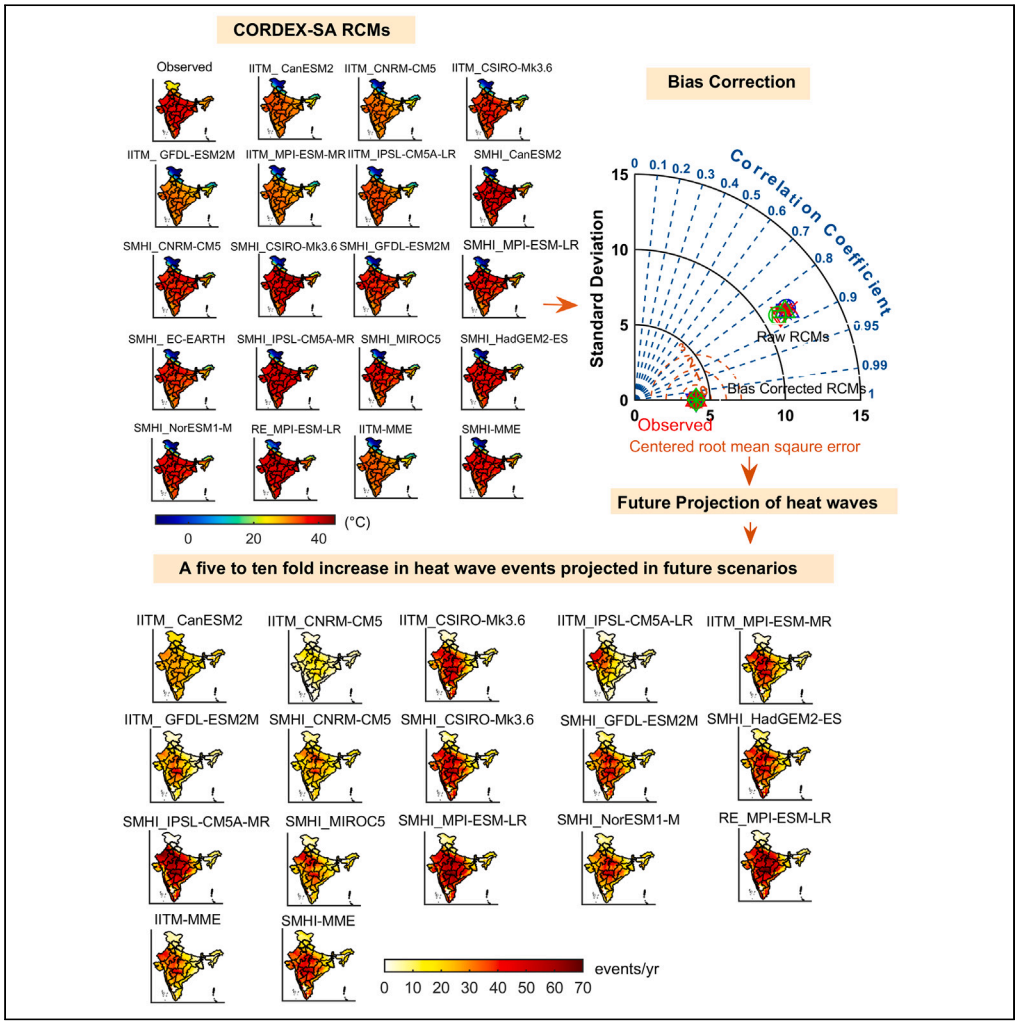

Saumya Singh, R.K. Mall

rkmall@bhu.ac.in

Highlights

Future increase in heat wave frequency will dominate intensity rise over India

Four-to-seven-fold and five-to-ten-fold increase under RCP 4.5 & RCP 8.5 scenario

South-Central India to observe largest increase in heat wave frequency in future

Increased risk of heat stress over the coastal region in future

Singh & Mall, iScience *26*, 108263
November 17, 2023
https://doi.org/10.1016/j.isci.2023.108263

iScience

CellPress
OPEN ACCESS

Article

Frequency dominates intensity of future heat waves over India

Saumya Singh[1] and R.K. Mall[1,2,*]

SUMMARY

Future changes in heat wave characteristics over India have been analyzed using Coordinated Regional Climate Downscaling Experiments (CORDEX) for South Asia (SA) regional climate model simulations for mid-term (2041–2060) and long-term (2081–2099) future under the representative concentration pathway (RCP) 4.5 and RCP 8.5 emission scenarios, respectively. SMHI_CSIRO-MK3.6 was found to be the best model in simulating heat wave trend over India for historical period. Future projections show a four-to-seven-fold increase in heat wave frequency for mid-term and long-term future under RCP 4.5 scenario, and five-to-ten-fold increase under RCP 8.5 scenario with increase in frequency dominating intensity in both the scenarios. Northwestern, Central, and South-central India emerged as future heat wave hotspots with largest increase in the south-central region. This high-resolution regional future projection of heat wave occurrence will serve as a baseline for developing transformational heat-resilient policies and adaptation measures to reduce potential impact on human health, agriculture, and infrastructure.

INTRODUCTION

An unequivocal influence of anthropogenic activities has resulted in an increase of 1.07°C in global mean surface temperature above preindustrial levels.[1] The widespread impact of the anthropogenic warming can be observed in the strengthening episodes of extreme weather events such as heat wave, droughts, forest fires, floods, etc., as well as irreversible long-term changes such as loss of biodiversity, ocean acidification, and sea ice melting, etc.[1] This increase is much pronounced at the regional level because with every degree rise in global temperature, the regional warming becomes larger.[1,2] Regional warming records show the increase to be of 1.5°C in at least one season in the regions where 20%–40% of global population lives; hence, regional assessments are crucial.[1]

Among the extreme weather events, heat waves have emerged as the most prominent tell-tale sign of climate change becoming more frequent, intense, and of longer duration in recent decades.[1] The most recent year 2022 observed unprecedented heat wave events exceeding previous thresholds with severe impacts for different regions of the world. These extreme temperature events have been found to have severe implications on health, agriculture, natural ecosystems, and infrastructure.[3–9] Studies on understanding the changing characteristics of heat waves have found the phenomenon to be driven by synoptic atmospheric circulations and intensified by regional land atmosphere interactions.[10–12] The delay of monsoon, low evaporative cooling, and depleted soil moisture increase the sensible heat flux and exacerbate the prevailing heat wave conditions.[8,12,13] Heat waves have emerged as an immediate health hazard increasing morbidity and huge mortality episodes across the globe such as during European heat wave of 2010 (70,000 deaths), Russian heat wave (54,000 deaths), and Indian heat wave of 2015 (>2,500 deaths).[11,14–16] India has reported a marked increase in heat wave intensity, frequency, and duration in the past half century.[8,11,17,18] Singh et al.[8] found a spatiotemporal shift in the heat wave events over India in the last seven decades which has given rise to the three heat wave hotspots of the country, i.e., Northwestern, Central, and South-Central India. During the recent unusual heat wave episode of 2022 Northwestern and Central India, two of these three hotspots experienced their hottest April in 122 years.[17] Zachariah et al.[19] reported that such episodes have become 30 times more likely due to climate change.

In such scenario, it becomes crucial to identify the future hotspots of heat wave in India which would require using high-resolution climate projections from state-of-the-art climate models. With the aid of Global Climate Models (GCMs), the scientific community has been able to simulate the characteristics of heat waves and other extreme weather events for historical and future scenarios.[18,20–24] While GCMs have found wide application in future projection studies, due to their coarse resolution they fail to capture the local dynamic changes that modulate climate signals at a regional scale. This inability of GCMs may limit their usage in impact assessment at a regional scale.[25,26] In order to study the regional impact of extreme weather events, robust information to detect local climate change signals is needed; hence, high-resolution regional climate projections are of vital importance.[26–28]

Dynamical downscaling using regional climate models (RCMs) is an efficient technique to study climate-related risk at a regional scale as they provide reliable data of climate parameters at a higher resolution.[26,29–31] Plavcová and Kyselý[32] stated an improvement in the simulation

[1]DST-Mahamana Centre of Excellence in Climate Change Research, Institute of Environment and Sustainable Development, Banaras Hindu University, Varanasi, India
[2]Lead contact
*Correspondence: rkmall@bhu.ac.in
https://doi.org/10.1016/j.isci.2023.108263

of atmospheric circulation by RCM over their driving GCMs. Application of RCMs provides the added value for generation of high-resolution climate information which GCMs are unable to provide.[31,33–35] Giorgi[31] stated that downscaled regional climate projections from Coordinated Regional Downscaling Experiment (CORDEX) are efficient for understanding and characterizing the regional to local climate phenomenon along with their variability and trends and have been widely explored to study the climatology, trends, extremes, and future projections of climatic variables over different domains of the world.[26,30,33,36–39] Molina et al.[40] studied future projections of heat waves using EURO-CORDEX RCM simulations over Mediterranean basin for representative concentration pathway (RCP) 4.5 and RCP 8.5 scenarios and found a large increase in the duration and intensity of heat waves for the 2071–2100 period.

Sanjay et al.[41] studied the future change in seasonal mean near-surface air temperature and precipitation over the Hindu Kush Himalayan region using thirteen CORDEX South Asia (SA) RCMs. The results show a high confidence and low uncertainty among downscaled RCMs in projecting the increase in precipitation intensity and warming by the end of 21st century under RCP 8.5 scenario. Choudhary et al.[37] reported an added value to climate projections by CORDEX-SA RCMs in the coastal regions of India with reduced bias in precipitation in the Western Ghats region. CORDEX SA datasets have been used to investigate the threshold crossing time for eight different warming targets over India between 1.5°C and 5°C using nine CORDEX-SA experiments.[42]

While the regional climate projections from CORDEX-SA datasets have been explored to study the climate of India, heat wave future projections using the dataset are yet to be done. Future projection of heat waves over India has been primarily studied using simulations from GCMs while large ensemble RCM-based studies are lacking.[5,38,43–45] Rohini et al.[46] projected an increase of an average two events and 12–18 days in duration of heat wave events over India during 2020–2064 under RCP 4.5 scenario with an increase of 0.5 event/decade and 4–7 days/decade in heat wave frequency and duration, respectively, over central India using Coupled Model Intercomparison Project (CMIP) 5 GCMs. Similarly, Mishra et al.[36] utilized seven GCM projections and projected future increase in severe heat waves over India to be 30 times higher than the present climate by the end of the 21st century. Dubey & Kumar[47] studied heat wave future projections over India using a single RCM projection and noted the limitations associated with projections from few RCMs and recommended application of large ensemble model-based assessment of heat wave over India for robust future projection. Hence, to address this gap of regional climate information-based robust assessment of heat wave over India, the present study is conceptualized and uses seventeen dynamical downscaled simulations from 3 RCM ensembles within CORDEX-SA framework to assess the model performances and future projection of changing characteristics of heat wave, i.e., frequency, intensity, and duration for mid-term (2041–2060) and long-term (2081–2099) future under RCP 4.5 and RCP 8.5 scenarios. This ensemble-based assessment will provide a range of possible heat wave trajectories and emerging future heat wave hotspots. The study will provide an added value to the present understanding and regional impact assessment of heat waves over India. Also, the findings of the model evaluation will pave way for improvement in individual model physics in simulating Indian heat wave climatology. The differences in downscaled simulations from the same GCMs due to use of different RCM for downscaling will be also useful for future CORDEX-SA downscaling initiatives from CMIP6 models.

RESULT

Performance evaluation of RCMs

Climatological mean (MEA-T)

The spatial distribution of model and observed climatological mean maximum temperature (MEA-T) and mean bias (MB) for March–June during climatological period of 1971–2000 were compared in the study to assess the model performance (Figures 1A and 1B). Both warm and cold bias is found to be associated with model simulations in comparison to the observed MEA-T range of 21.90°C–39.32°C. Indian Institute of Tropical Meteorology (IITM) ensemble models showed a clear underestimation of mean temperatures with an inter-ensemble variation of −11.79°C (IITM_GFDL-ESM2M) to 37.09°C(IITM_CSIRO-Mk3) where the Commonwealth Scientific and Industrial Research Organization (CSIRO) model IITM_CSIRO-Mk3 model was found to be the best among the suit with much lower bias than other models.

The Swedish Meteorological and Hydrological Institute (SMHI) ensemble models showed much lower bias than IITM ensemble models (Figure 1B) and simulated mean temperature closer to observation except for the northern mountainous regions; the MEA-T range varies from −14.67°C (SMHI_GFDL-ESM2M) to 41.76°C (SMHI_CSIRO-Mk3). However, the maxima of MEA-T mean temperature in IITM ensemble RCM were found to be spatio-temporally closer to the observation with lower mean bias (warm) in maxima ranging between 0.08°C (IITM_GFDL-ESM2M) to +2.54°C (IITM_CSIRO-Mk3) whereas the SMHI ensemble RCMs overestimated the maxima by +8.28°C (SMHI_IPSL-CM5A-MR). RE_MPI-ESM-LR showed the largest variation with both the highest cold and warm bias of −31.86°C and 8.28°C, respectively. Among the multi-model ensemble (MME) means the SMHI_MME captured the maxima (39.09 C) better than IITM_MME (34.65 C). However, the overall area average mean bias showed that IITM ensemble RCMs underestimated the climatological mean while the SMHI ensemble was better in approximating the observed temperature (Table 1).

Spatio-temporal variability and probability distribution. Taylor diagram summarizes the model performance in simulating long-term spatial mean temperature over India (Figure 2). The inter-model spread for Root-mean-square error (RMSE) among the ensembles shows IITM ensemble have comparatively higher RMSE (8.38–11.07) against SMHI ensemble (8.62–9.16) but higher pattern correlation coefficient (~0.9) against the SMHI ensemble (0.86) before bias correction. Bias correction significantly improves in mean temperature simulations with RMSE and mean absolute error (MAE) being reduced to zero while index of agreement and correlation increasing to 1 for all the RCM simulations. Table 2 depicts the results of model performance metrics and mean values before and after bias correction and shows that mean and variance of the individual models and MME mean are same as the observed.

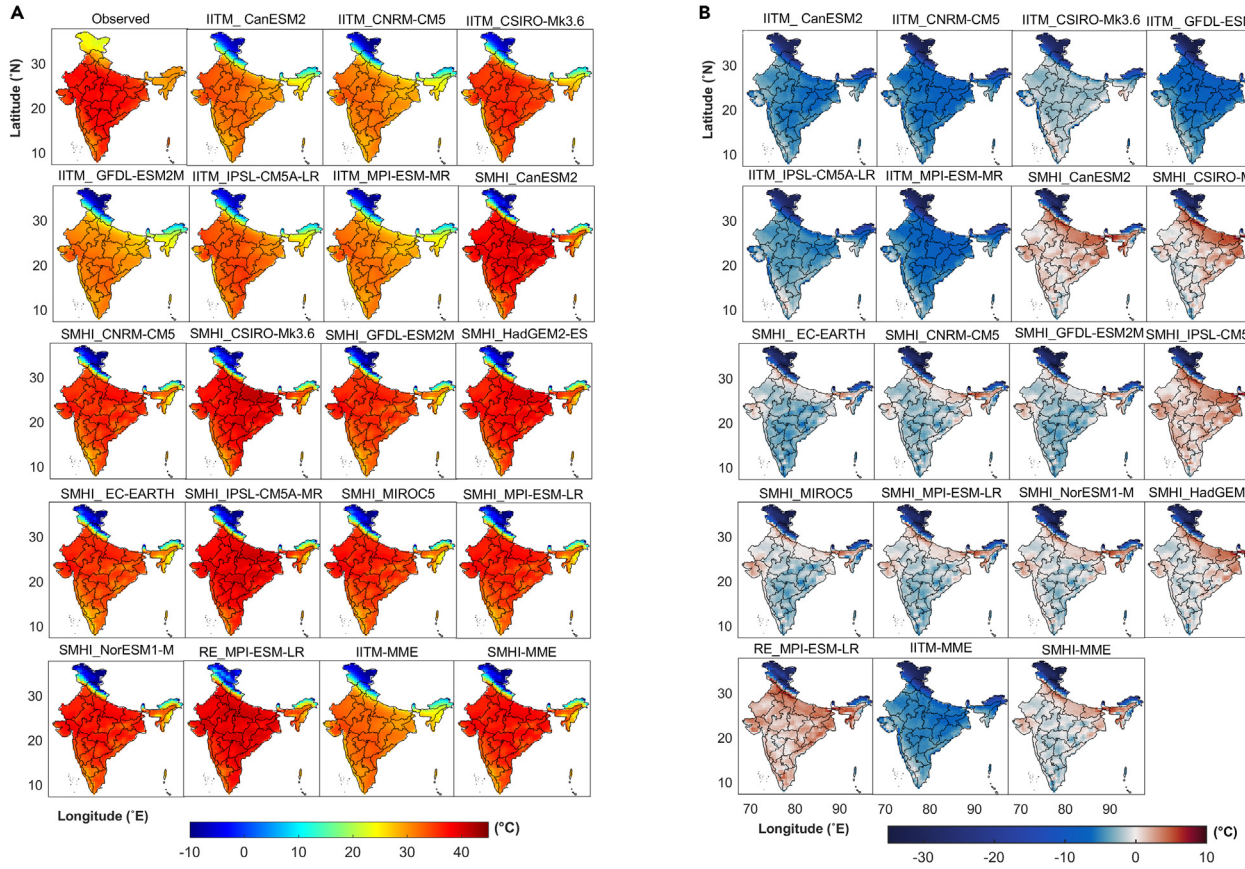

Figure 1. Climatological mean maximum temperature over India

(A) Climatological mean maximum temperature simulated by CORDEX-SA RCMs over India for Mar–Jun (1971–2000).

(B) Mean bias simulated by CORDEX-SA RCMs over India for Mar–Jun (1971–2000).

The non-parametric kernel density estimate (KDE) distribution with a kernel bandwidth of 0.5, representing a higher fidelity of probability density distributions of maximum temperature, is assessed for model simulations against observation (Figure 3). The distribution shows comparatively larger variation in location parameter from 35°C (observed) to around 32°C for the IITM ensemble members (represented by different shades of blue in Figure 4) while showing lower variation with ∼34°C for SMHI ensemble (represented by different shades of red in Figure 4). The added advantage of variance scaling is reflected in the KDE as all RCM simulations approximated the scale, location, and shape parameter of the distribution similar to observation. IITM_CSIRO (−5.22°C–51.71°C), IITM_MPI-ESM (−2.61°C to 53.45°C) of the IITM ensemble and SMHI_HadGEM2-ES (−2.16°C–51.23°C), SMHI_EC-EARTH (−3.87 to 52.24) of SMHI ensemble showed better agreement with the observation. Also, the IITM_MME (−0.58°C–52.08°C) and SMHI_MME (−3.06°C–51.40°C) showed better daily temperature distribution among all model simulations. Similarly, the improvement after bias correction can be seen in the empirical cumulative distribution function (ECDF) (Figure 3B) where all RCMs simulated the temperature in the observed distribution after bias correction.

Temperature extremes

The model performance in simulating very warm day threshold (TX95t) and seasonal maximum value of daily maximum temperature (TXx) is assessed where three ensemble outputs and their MME means before and after bias correction have been assessed (Figures 1 and 4). It is observed that before bias correction all of the models have underestimated both the indices recording temperatures as low as −4°C in the mountainous region due to existing cold bias in the model. Over other parts of the country IITM ensemble models underestimate the indices (∼2°C–3°C) while SMHI ensemble models overestimate the indices (∼4°C–5°C). After bias correction the indices show similar spatial patterns and magnitude of TX95t thresholds corresponding to observed patterns with a ∼±0.5°C variation from the observed mean value of 44.87°C after bias correction (Figure 4). However, the TXx index reflects the differences in extreme temperature simulation where an overestimation of +4°C to +10°C was observed among the IITM ensemble member simulating higher extremes in the Central, South-Central, and eastern coastal region of the country which are also among the most heat wave vulnerable regions.[47]

Table 1. Mean, standard deviation (SD), root-mean-square error (RMSE), mean absolute error (MAE), and index of agreement (d) of raw (mod) and bias-corrected (var) model data datasets for long-term mean maximum temperature in historical period (1971–2005)

	Mean		SD		MAE	RMSE	PBIAS	d
	IMD = 34.69		IMD = 4.08		Var = 0	Var = 0	Var = 0	Var = 1
RCM	(Mod)	(Var)	(Mod)	(Var)	(Mod)	(Mod)	(Mod)	(Mod)
IITM_CNRM-CM5	26.62	34.69	10.14	4.08	8.07	10.52	−23.3	0.6
IITM_CanESM2	27.79	34.69	9.68	4.08	6.89	9.31	−19.9	0.64
IITM_CSIRO-Mk3	30.22	34.69	10.55	4.08	4.55	8.38	−12.9	0.69
IITM_IPSL-CM5A-LR	28.57	34.69	10.16	4.08	6.13	9.08	−17.6	0.66
IITM_MPI-ESM-MR	26.56	34.69	9.93	4.08	8.12	10.47	−23.4	0.6
IITM_GFDL-ESM2M	26.19	34.69	10.39	4.08	8.49	11.03	−24.5	0.59
RE_MPI-ESM-LR	34.32	34.69	11.03	4.08	4.3	7.78	−1.1	0.72
SMHI_HadGEM2-ES	32.43	34.69	11.79	4.08	4.03	8.86	−6.5	0.68
SMHI_CNRM-CM5	30.70	34.69	11.48	4.08	4.49	9.16	−11.5	0.66
SMHI_CanESM2	33.41	34.69	11.80	4.08	4.17	8.62	−3.7	0.69
SMHI_CSIRO-Mk3	33.25	34.69	11.62	4.08	4.16	8.48	−4.1	0.7
SMHI_GFDL-ESM2M	30.38	34.69	11.53	4.08	4.65	9.34	−12.4	0.65
SMHI_IPSL-CM5A-MR	33.64	34.69	12.08	4.08	4.4	8.87	−3	0.68
SMHI_MIROC5	31.03	34.69	11.21	4.08	4.2	8.75	−10.5	0.68
SMHI_MPI-ESM-LR	31.22	34.69	11.30	4.08	4.18	8.77	−10	0.67
SMHI_NorESM1-M	31.54	34.69	11.70	4.08	4.06	9.03	−9.1	0.67
SMHI_EC-EARTH	30.14	34.69	11.03	4.08	4.84	9.04	−13.1	0.66
IITM_MME	27.66	34.69	10.12	4.08	7.03	9.72	−20.3	0.63
SMHI_MME	31.77	34.69	11.54	4.08	3.94	8.78	−8.2	0.68

The only model that approximates the observed pattern with lower warm bias is IITM_CSIRO-MK3. The SMHI ensemble models show relatively better spatial variability with a lower underestimation of +2°C to +7°C than observation among which SMHI_EC-EARTH, SMHI_HadGEM2-ES, and SMHI_GFDL-ESM2M capture the spatial patterns and extreme value closer to the observation. Similarly, the SMHI_MME mean simulated the TXx better both spatially and in mean within a range of 34.85°C–50.47°C than IITM_MME (35.33°C–51.13°C). RE_MPI-ESM-LR showed the highest overestimation of +12°C with extreme values reaching 59.83°C over a few grids in the northern region.

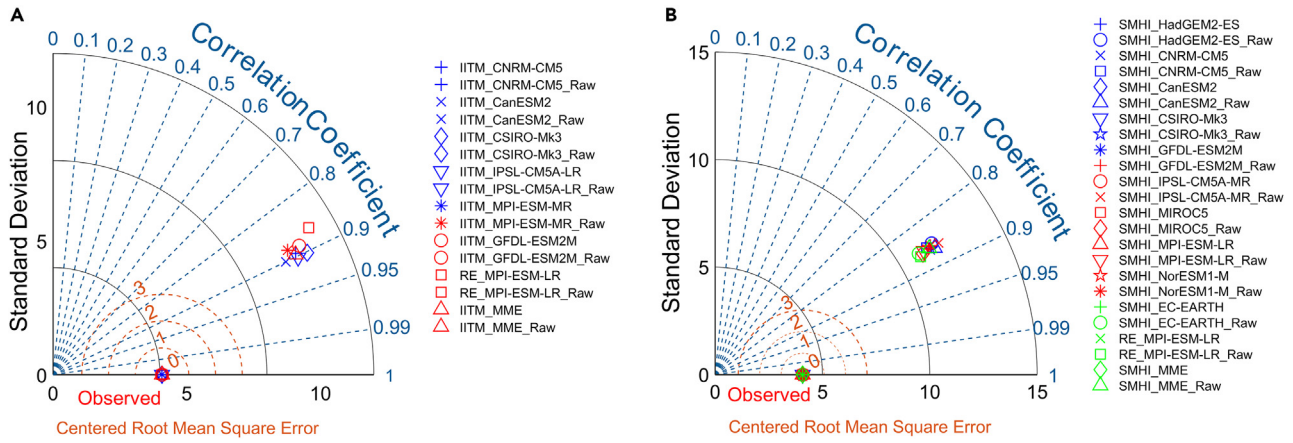

Figure 2. Taylor diagram of CORDEX-SA RCMs

(A) Taylor diagram showing model performance of CORDEX-SA IITM ensemble RCMs before and after bias correction.

(B) Taylor diagram showing model performance of CORDEX-SA SMHI ensemble RCMs before and after bias correction.

Table 2. Mean change in maximum temperature over India for mid-term (2041–2060) and long-term future (2081–2099) under RCP 4.5 and RCP 8.5 scenario

	RCP 4.5		RCP 8.5	
RCM	Mid- term (2041–2060)	Long-term (2081–2099)	Mid- term (2041–2060)	Long-term (2081–2099)
IITM_CNRM-CM5	1.31	1.67	1.84	2.54
IITM_CanESM2	1.69	2.09	2.05	3.71
IITM_CSIRO-Mk3	2.58	3.24	2.34	4.98
IITM_IPSL-CM5A-LR	1.44	1.77	1.79	3.29
IITM_MPI-ESM-MR	2.02	2.35	2.35	4.72
IITM_GFDL-ESM2M	1.64	2.16	1.91	3.65
RE_MPI-ESM-LR	2.06	2.54	2.39	5.73
SMHI_EC-EARTH	1.93	–	2.20	–
SMHI_CNRM-CM5	1.76	2.13	2.06	3.58
SMHI_CanESM2	2.20	2.94	2.99	–
SMHI_CSIRO-Mk3	2.28	3.11	2.41	4.95
SMHI_GFDL-ESM2M	1.82	2.23	1.91	4.16
SMHI_HadGEM2-ES	2.06	2.95	2.57	4.86
SMHI_IPSL-CM5A-MR	2.26	3.5	3.03	6.09
SMHI_MIROC5	2.06	2.35	2.59	4.33
SMHI_MPI-ESM-LR	2.06	2.39	2.47	5.52
SMHI_NorESM1-M	1.85	2.26	2.33	4.33
SMHI_MME	2.13	2.93	2.56	4.83
IITM_MME	1.86	2.29	2.12	4.43

The highest changes in each scenario are highlighted by shading.

Heat wave events

The spatial distribution of frequency, intensity, and duration for the average heat wave events/year during Mar-June (1971–2005) is assessed (Figure 5). The highest number of heat wave (HW) events are observed in northern, northwestern, central, and south-central region of the country with no HW being observed in the south-western region of the country. All of the RCMs successfully simulate heat wave in these regions which affirms their ability in capturing the regional features of the plain, hilly, and coastal regions of India. RE_MPI-ESM-LR underestimates the frequency of the heat wave events. The zones of maximum heat wave frequency are best reproduced by the IITM_CSIRO-Mk3.6 and IITM_GFDL-ESM2M from IITM ensemble and SMHI_CSIRO-Mk3.6, SMHI_IPSL-CM5-MR, and SMHI_EC-EARTH from SMHI ensemble. Further, SMHI_NorESM1-M and SMHI_HadGEM2-ES also capture the spatial variability with lesser overestimation than other models. IITM_CNRM-CM5 overestimates the spatial occurrence and frequency of heat wave events reaching up to 8 events/year in most of the northern-northwestern, central, south-central, and eastern region making it the most unreliable model to study heat waves over India. The MME means are found to simulate heat wave zones reasonably well among all the models with slight overestimation in the frequency. The overestimation can be attributed to the excess heat wave events simulated by the ensemble members. The maximum intensity of heat wave events is observed over the Northwestern, Central, and South-central region reaching up to 47°C while the minimum intensity is observed to be 32.4°C over the western coast and northern hilly areas.

In the IITM ensemble it was observed that IITM_CSIRO-Mk3.6 captures both the spatial variability and the intensity range best followed by IITM_IPSL-CM5A-LR and IITM_CNRM-CM5, while IITM_CanESM2, IITM_MPI-ESM-MR, and IITM_GFDL-ESM2M overestimated the intensity of heat wave events reaching up to 52°C–56°C. The overestimation is mainly observed over the central and eastern region consisting of Odisha, West Madhya Pradesh, Chhattisgarh, Vidarbha, and Telengana region. As these regions fall into heat wave-prone zones,[8] this overestimation of intensity (3°C–5°C) must be considered when making future projections. SMHI ensemble models reproduced both the spatial occurrence and magnitude of the intensity better than IITM ensemble and are closer to the observation with intensity between 30°C and 49°C. The intensity simulated by SMHI_CSIRO-Mk3.6, SMHI_IPSL-CM5A-MR, and SMHI_EC-EARTH corresponds to the observation most closely. RE_MPI-ESM-LR underestimated the intensity in the eastern region of the country. Both the MME means capture the spatial variability and range of the intensity well sparing an overestimation in the central region (Western Madhya Pradesh) by the IITM MME mean. The boxplot in Figure S5 shows distribution of heat wave intensity for historical period where the quartile range and median intensity of SMHI ensemble models and both MME means are found to be more consistent with the observation than IITM ensemble models observing 1°C–2°C higher median intensity.

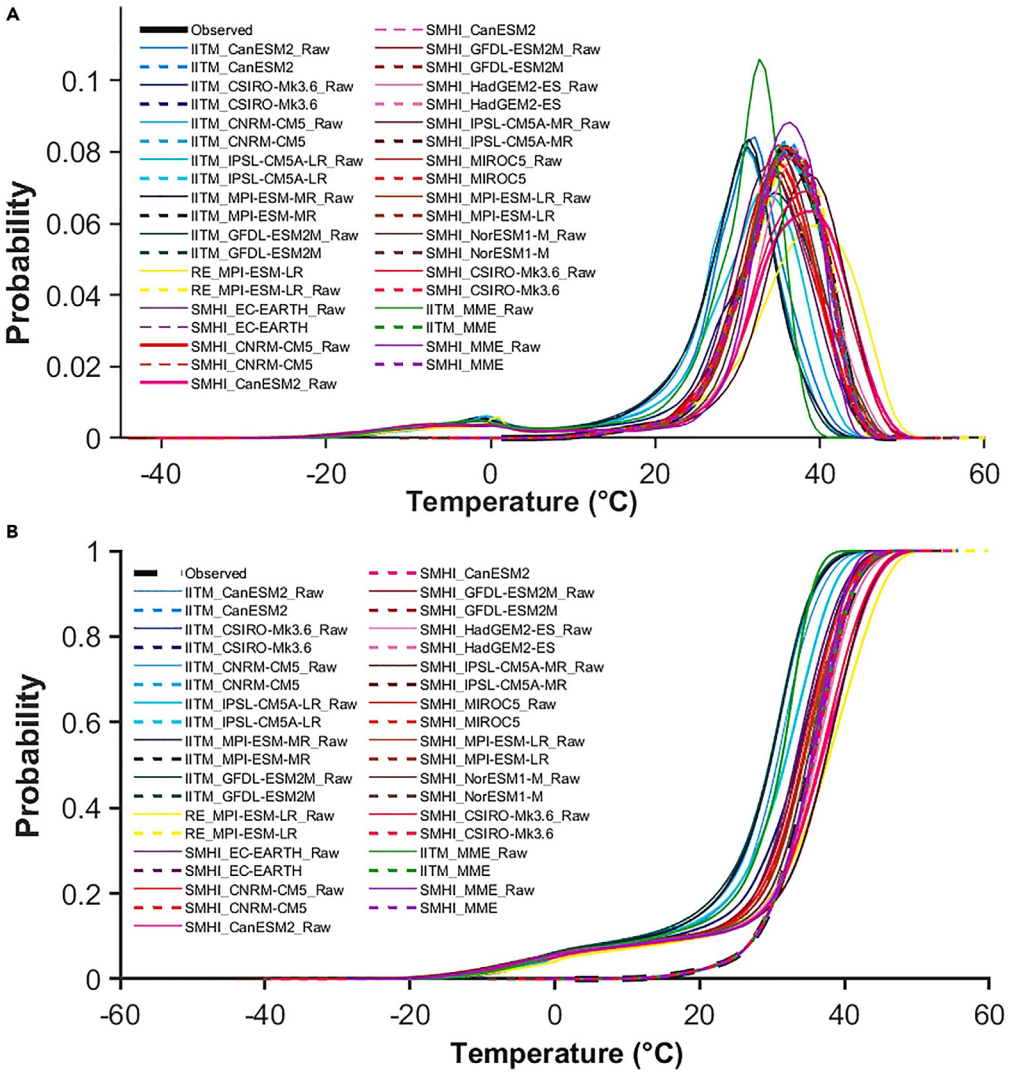

Figure 3. Probability density distribution of daily maximum temperature

(A) Kernel Density estimate distribution of CORDEX -SA RCMs before and after bias correction.

(B) Empirical Cumulative frequency distribution of CORDEX- SA RCMs before and after bias correction.

The third characteristic is duration which exacerbates the impact of the heat wave causing morbidity and mortality in case of prolonged duration.[5] Figure 5C shows that the HW duration ranges from 2 to 18 days with the longest duration over the northern and Central India. IITM_CanESM2, which overestimated intensity, overestimates the duration in the central, eastern, and south-central region while underestimating in the northern region with an average of 4–6 days. IITM_CSIRO and IITM_IPSL-CM5A-LR approach the observation better than other models of the ensemble. Similarly, for SMHI ensemble, SMHI_CSIRO-Mk3.6 and SMHI_IPSL-CM5A-MR appear closer to the observation while the SMHI_CanESM2, SMHI_MIROC, and SMHI_GFDL-ESM2M overestimate the duration over most of the region of the country. IITM MME mean simulated duration in the heat wave-prone zones is better than SMHI MME mean. Figure S5 shows boxplot distribution of duration for historical period which presents nearly similar distribution and median duration simulated by all RCMs as compared to the observed.

Trend analysis

A significantly increasing trend of 0.2 events/yr over the western, central, and south-central region of the country is observed while a significantly decreasing trend ranging between −0.1 and −0.2 events/year over the eastern region of the country (Figure S2) is observed. These results correspond to the earlier studies by Singh et al.[8,28] where similar significant increase and decrease were observed in the regions. The trends observed by the model simulations varied in spatial occurrence and magnitude. While majority of the IITM ensemble models observed an increasing trend in the northwestern and central region of the country with an overestimation of 0.1–0.2 events/year, the decrease in the eastern region was not reproduced by any of the models. Among all the models, IITM CanESM2 captured the spatial

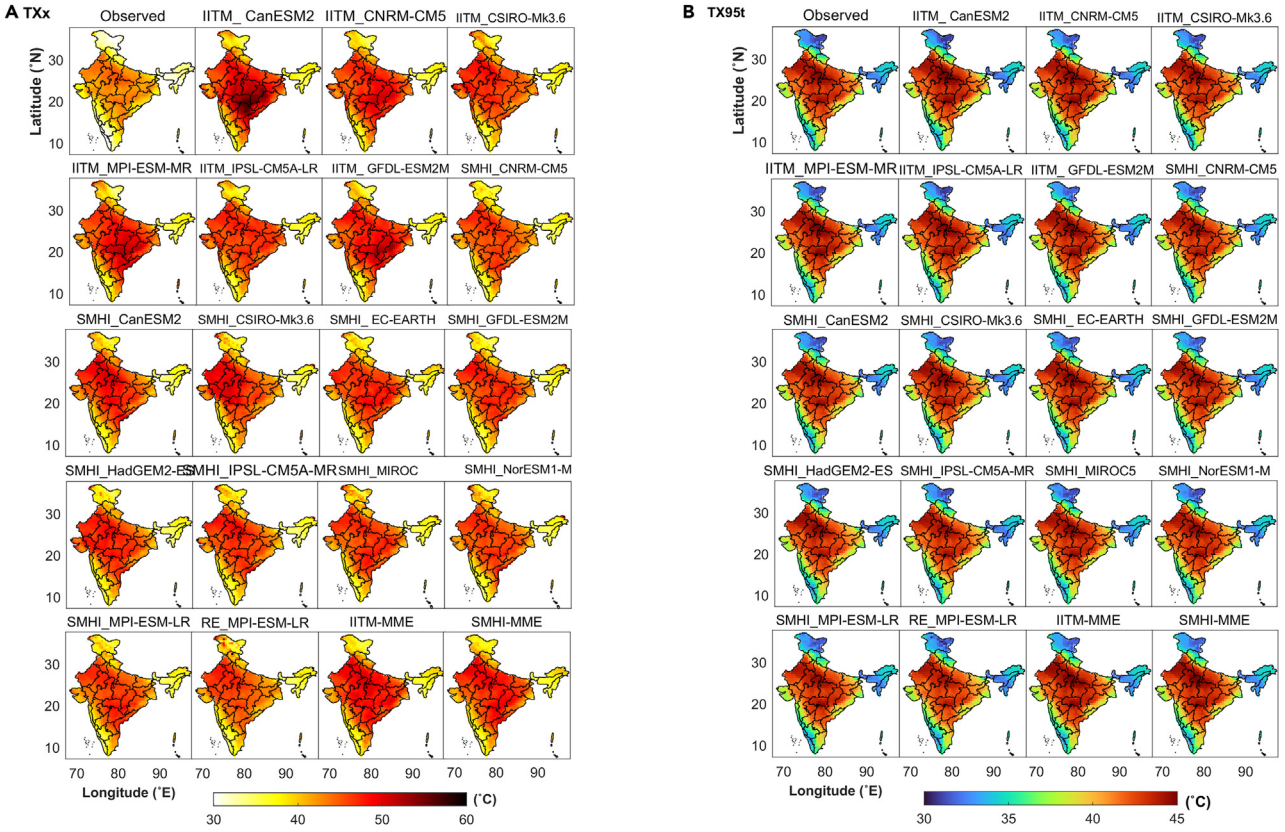

Figure 4. CORDEX-SA RCM simulated climate impact indices

(A) TXx simulated by CORDEX-SA RCMs after bias correction.

(B) TX95t simulated by CORDEX-SA RCMs after bias correction.

occurrence of HW events in Western Rajasthan and Western Madhya Pradesh while IITM IPSL-CM5-LR overestimated both the spatial occurrence and frequency of heat wave events over these regions and decrease in the south-eastern region comprising Odisha and Rayalseema. Among the SMHI ensemble models that overestimate both the spatial occurrence and frequency of events, SMHI CSIRO-Mk3.6 shows similar trend as observed in western, northwestern, and central India with a significant increase of 0.2 event/year and a decrease of −0.5 events/year in the eastern region. SMHI GFDL-ESM2M, SMHI_MIROC, and SMHI_NorESM1-M also simulate the increasing trend closer to the observation. All of the SMHI models show a consistent increasing trend in the northern region consisting of the Uttarakhand and Shimla against the negative trend shown in observation. RE_MPI-ESM-LR also follows the pattern observed by the SMHI ensemble members. Both the MME means overestimate the frequency and spatial occurrence of heat wave events recording an increase of 0.4 events in the northern, northwestern, central, and south-central region, but IITM MME mean performs better than the SMHI MME mean.

Future changes in maximum temperature

Future changes in maximum temperature has been assessed in the study prior to heat wave projections to identify the pattern of future temperature evolution (Figures S3 and S4). Over India, a mean change of 1.31°C–2.58°C (mid-term) and 1.67°C–3.54°C (long-term) under RCP 4.5 scenario and 1.79°C–3.03°C (mid-term) and 2.54°C–6.09°C (long-term) under 8.5 scenario (Table 2) was observed, which vary spatially for different regions (Figures S3 and S4). Northern, Northwestern, and Central India may observe an increase of 2.5°C (mid-term) to 4°C(long-term) projected by SMHI_IPSL-CM5A-MR and SMHI_CSIRO-Mk3.6, as well as eastern and southern region projected by IITM_ CSIRO-Mk3.6 and RE_MPI-ESM-LR under RCP 4.5 scenario. The regions will further observe a rise of ~4°C (mid-term) to ~6°C (long-term) under RCP 8.5 scenario with highest increase of ~8°C simulated by SMHI_IPSL-CM5A-MR over the northern region. IITM ensembles RCMs simulate higher changes than SMHI ensemble RCMs and RE_MPI-ESM-LR for long-term future. The respective MME mean follows the pattern displayed by the ensemble models.

Heat waves projections over India

Future projection of heat waves over India has been assessed for mid-term (2041–2060) and long-term (2081–2099) future under RCP 4.5 and 8.5 scenario (Figure 6). For RCP 4.5 scenario, a 4- to 7-fold increase in heat wave events is projected over India with a maximum of

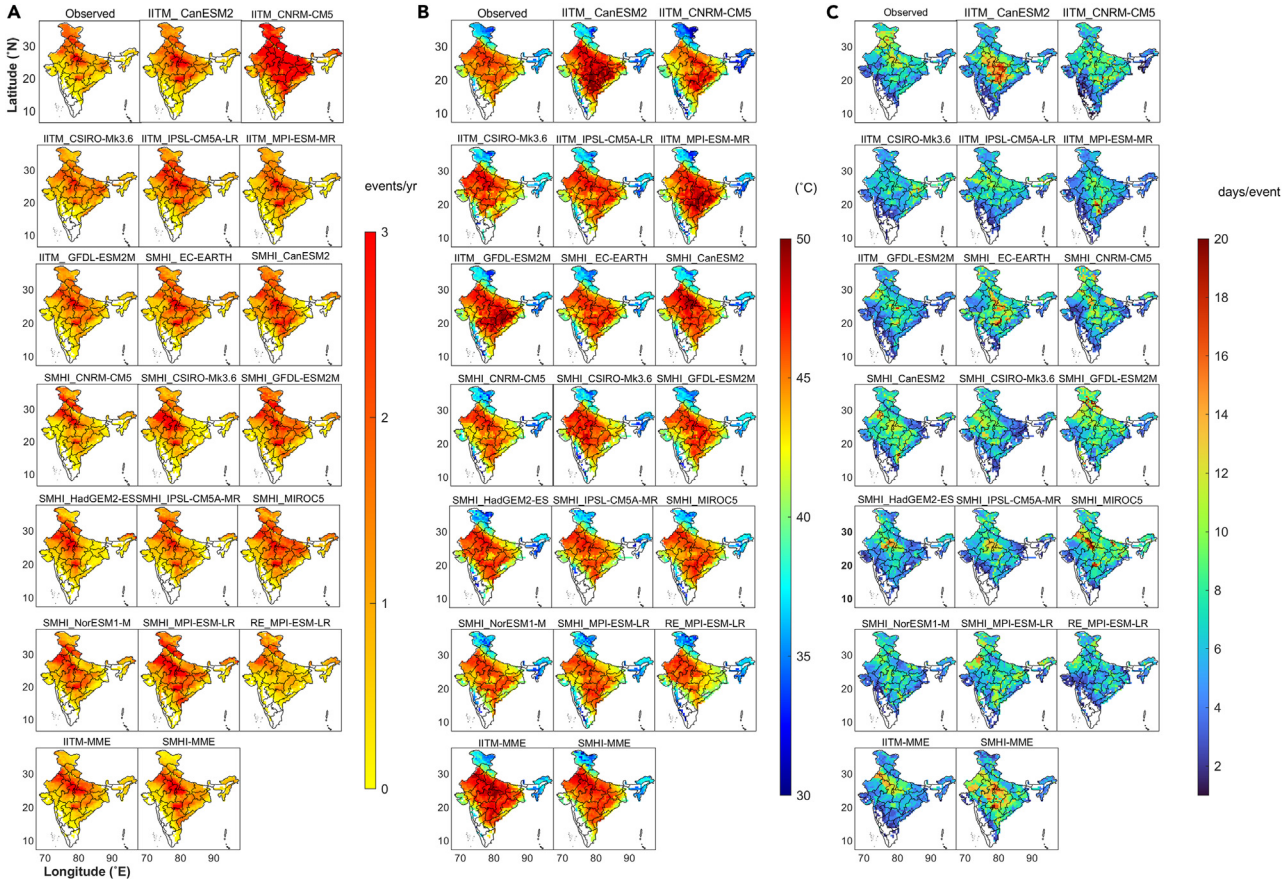

Figure 5. Evaluation of heat wave characteristics over India

(A) CORDEX SA -RCM simulated frequency of heat wave events over India during MAMJ (1971–2005).

(B) CORDEX SA -RCM simulated intensity of heat wave events over India for Mar–Jun (1971–2005).

(C) CORDEX SA -RCM simulated duration of heat wave events over India for Mar–Jun (1971–2005).

20 events/year during mid-term future to further 35 events/year for the long-term future. CSIRO-Mk3.6 which performed better among all models during evaluation in both the ensembles projects the highest frequency of 20 events/year in northwestern, central, and south-central region. While most of the IITM ensemble models and ensemble mean project an increase of 2–12 events/year, the SMHI ensemble projects a higher maximum of 15–20 events/year. RE_MPI-ESM-LR also observed the highest frequency of 20 events/year but differed from other models in the region of maximum frequency which was south-central region only.

The spatial variability shows heat waves to occur all over India with most pronounced in the northern and central region including east and west Rajasthan, East Madhya Pradesh, West Madhya Pradesh, and Vidarbha. The coastal region which records high mortality due to presence of humidity and low diurnal temperature range in case of extreme temperature and heat waves exhibits an increase of 4–6 events/year in future which can aggravate the heat stress condition.[8] Heat wave events are found to recede from the southern region particularly south-western coastal region in long-term future as projected by most of the models. However, the frequency of heat wave increased in rest of the country showing a higher distribution reaching more than 35 events/year as simulated by CSIRO-Mk3.6 and SMHI-IPSL-CM5-MR. While these two models simulated the maximum frequency, remaining models project an average of 20–25 events/year all over the country.

For RCP 8.5 scenario that represents a 3-fold higher greenhouse gas emission scenario and so a higher increase in temperature extremes, heat wave events show a five-to-ten-fold increase in mid-term (2041–2060) to long-term period (2081–2099) over the country (Figure 7). The increase is consistent in the regions that showed increase in the RCP 4.5 scenario with a varying magnitude. The frequency estimated by the SMHI ensemble models is higher (25–30 events/year) than that estimated by the IITM ensemble model (15–20 events/year) except for IITM_CSIRO-Mk3.6 and IITM_MPI-ESM-MR (25 events/year). An increase in heat wave over entire India can be observed with most of the country under heat wave occurrence in RCP 8.5 scenarios. IITM_CSIRO-Mk3.6, SMHI_CSIRO-Mk3.6, SMHI_GFDL-ESM, SMHI_MIROC, and SMHI_NorESM1-M, which showed better performance for the historical trends, project an increase of around 35–60 events/year with the highest frequency in the south-central, northwestern, central, and western region of the country. The southern region can be also seen recording

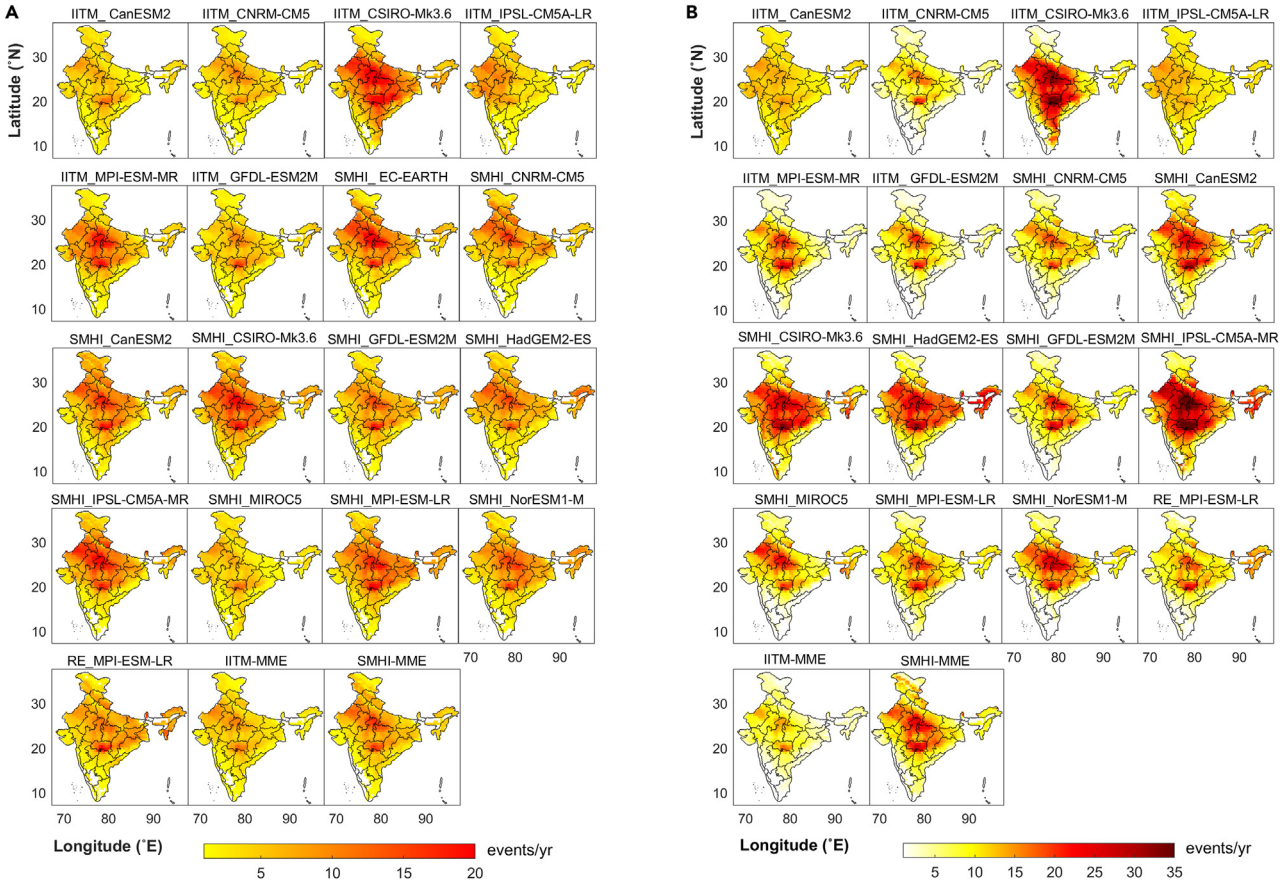

Figure 6. Future heat wave projections under RCP 4.5 scenarios

(A) CORDEX-SA RCM simulated heat wave events/year during Mar–Jun for mid-term future (2041–2060) under RCP 4.5 scenario.

(B) CORDEX SA -RCM simulated heat wave events/year during Mar–Jun for long-term future (2081–2099) under RCP 4.5 scenario.

more events. However, IITM_CanESM2 which simulated heat wave similar in the northwestern and central region for the evaluation period varies largely from the other models recording 20–30 events/year in those regions, whereas SMHI_IPSL-CM5-MR, SMHI_MPI-ESM-LR, and RE-MPI-ESM-LR project 50–70 events/year over the country except the northern region. The results for the RCP scenarios show that there will be a consistent increase in heat wave events over India with south-central region becoming warmer than any other part of the country followed by Northwestern and Central India making them future heat wave hotspots as well.

The best estimate of average heat wave events frequency and change simulated by all seventeen RCM datasets over India is estimated through boxplot distribution (Figure 8). For RCP 4.5 mid-term (R4 F1) and long-term (R4 F2) scenario heat wave events may observe a median increase of 4–6 events whereas for RCP 8.5 mid-term (R8 F1) and long-term (R8 F2) scenario a change (increase) of 6–20 events may occur from historical period. Average frequency of heat wave events is projected to rise to a median ~5 to 7 events and ~7 to 20 events in RCP 4.5 and RCP 8.5 mid-term and long-term future, respectively. Figures S5 and S6 shows the uncertainty in the distribution of historical and future heat wave intensity and duration over India.

A gradual increase in the median intensity from around ~46°C in historical period to ~49°C (RCP 4.5) to ~50°C (RCP 8.5) by IITM ensemble RCMs and ~48°C (RCP 4.5) to ~49°C (RCP 8.5) by SMHI ensemble RCMs in the long-term future shows a consistent difference of 1°C in median intensity between ensembles. The IITM models project the higher maximum intensity within the range of ~54°C–~59°C while SMHI ensemble and ensemble mean show lower maximum intensity of ~51°C–~54°C. For duration, all RCMs showed an agreement with the observation in historical period but showed large inter-ensemble spread in both mid-term and long-term future. Most of the models in both the ensemble show a median maximum duration range of 12–18 days (RCP 4.5) and 13–22 days (RCP 8.5) mid-term future which increases to 15 to 22 days (RCP 4.5) and 30 to 51 day (RCP 8.5) in long-term future. However, some of the models and the ensemble means project a larger increase with maximum duration of 56 days (IITM_CanESM2) and 67 days (SMHI EC-EARTH) in mid term to 77 days (RE_MPI-ESM-LR) in long term under RCP 8.5 scenarios. Similar increase in the intensity and duration in heat wave events over India has been projected by Dubey & Kumar[47] for far future period under RCP 8.5 scenario. However, they recommended the use of ensemble of models for a realistic projection of heat waves which the present study provides for all three characteristics of heat wave over India.

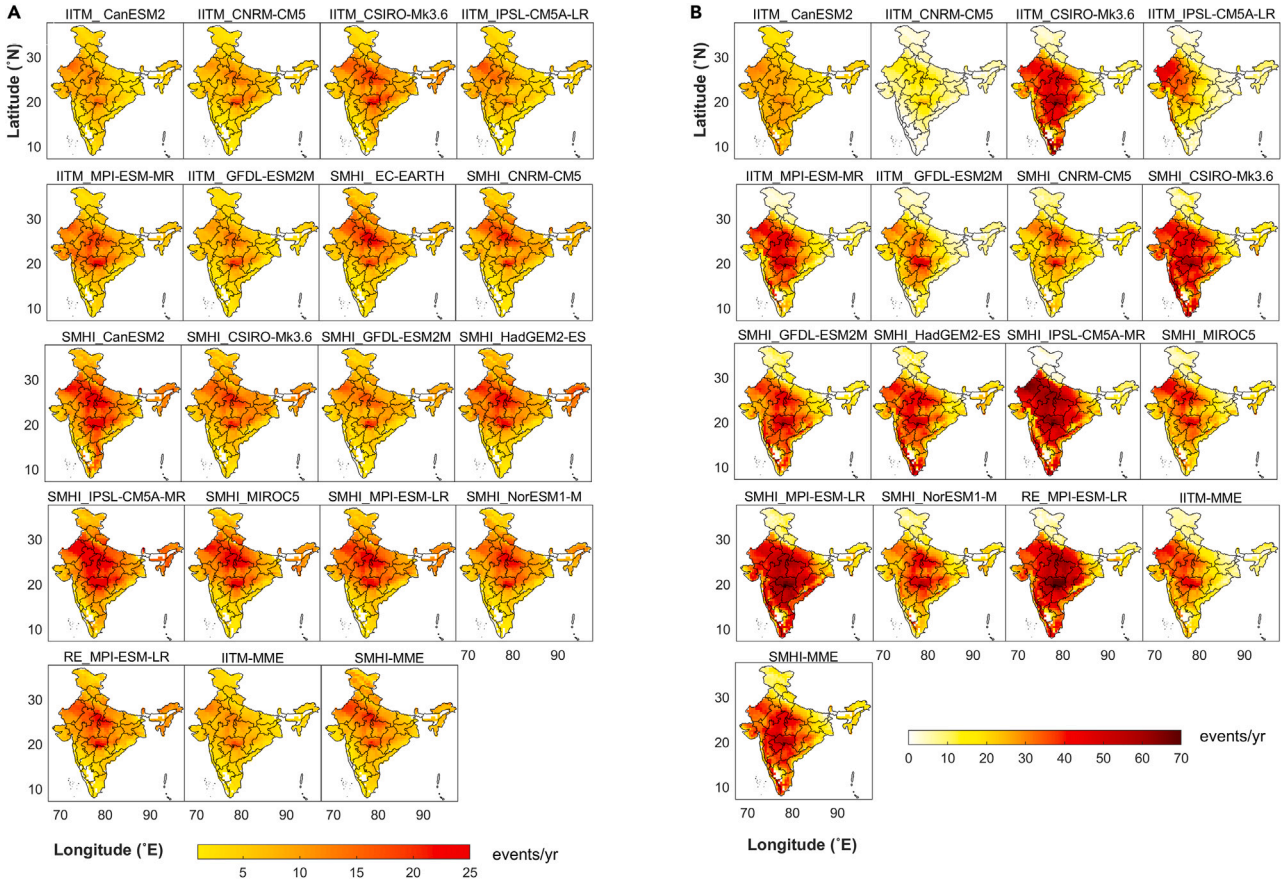

Figure 7. Future heat wave projections under RCP 8.5 scenarios

(A) CORDEX-SA RCM simulated heat wave events/year during Mar–Jun for mid-term future (2041–2060) under RCP 8.5 scenario.

(B) CORDEX SA -RCM simulated heat wave events/year during Mar–Jun for long-term future (2081–2099) under RCP 8.5 scenario.

DISCUSSION

Before simulating future projections, model performance evaluation was carried out in simulation of maximum temperature, extremes, and heat wave events which showed the varied performances of RCMs in comparison to the observation. A cold bias (underestimation) in the northern hilly region is observed for all RCM simulations, and warm bias was reported in the central and eastern region of the country. Similar warm and cold bias has been reported by Prajapat et al.[42] in evaluating the CORDEX-SA experiments for projecting future spatiotemporal warming over India.[45,48] The warm bias/overestimation over the country particularly in the eastern and some parts of central India as can be seen in the simulation of climatological mean and climate impact indices (TXx and TX95t) can be attributed to the dry bias in the central region due to loss of moisture from the atmosphere as well as the positive bias in temperature over the Bay of Bengal region.[37,45,48] The underestimation in the maximum temperature (cold bias) over the Himalayan region has been reported by several studies CORDEX-SA RCMs as well as their driving GCMs.[28,45,49–52] To explain the cold bias it is observed that the Himalayas exhibit complex topography and dynamic weather variability and hence are difficult to characterize using either GCMs or RCMs.[52,53] Mishra et al.[50] reported an underestimation (cold bias) of 10°C–15°C in the northern and northeastern region of India in the multi-model-mean of CMIP5 GCMs which are also the driving GCMs for the CORDEX RCMs, and the underestimation is similar to the underestimation reported in the present study. Sanjay et al.[42] observed an underestimation of more than 2°C in mean temperature over the Hindu Kush Himalayan region during summer monsoon season by the MME of CORDEX driving Atmosphere-Ocean coupled General Circulation Models (AOGCMS) but found that CORDEX multi-RCMs provide better confidence in projecting seasonal warming in the Himalayan region than their driving AOGCMs and so recommended their future application. A number studies on the Himalayan region using CORDEX-SA RCMs have acknowledged the limitation of model performance in the Himalayan region owing to regional topography, systemic biases, wet bias, individual model physics, overestimation, etc.[51,51,53–57]

Nayak et al.[53] and Prajapat et al.[42] noted similar significant cold bias in the northern region by RegCM4 simulations and CORDEX-SA experiments, respectively, during summer season. Nengker et al.[54] assessed the performance of CORDEX-SA RCMs in simulating mean temperature over Himalayan region and found similar cold bias in the Himalayas but made a note on the capacity of the RCMs to capture the temperature gradient with topography as the Northwestern Himalayas being at the highest elevation and colder than lower and eastern

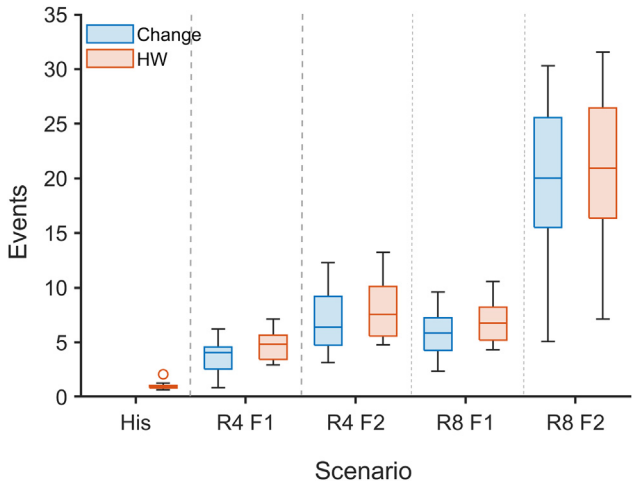

Figure 8. Boxplot showing future heat wave frequency and change in heat wave events over India from historical to mid-term (2041–2060) and long-term (2081–2099) future scenario under optimistic and pessimistic scenario shown as His, R4 F1, R4 F2, R8 F1, and R8 F2 in the figure.

Himalayas. Nayak et al.[53] attributed the cold bias to high water availability and less surface energy computations associated with the parameterization schemes used in the models and so pointed out the need to accommodate the associated processes to improve the model performances. Mishra et al.[50] concluded that the cold bias is a systemic bias associated with all of the models and does not depend on resolution but the parameterization schemes. Kotlarski et al.[33] explained the cold bias reported by CNRM RCM simulations over high mountains from EURO-CORDEX was due to the snow scheme and persistent snow cover. Haslinger et al.[58] found that the cold bias can also be attributed to the wet bias in the models due to overestimation of snow cover, moisture, and evaporation feedbacks in the CORDEX-SA experiment, which have also been reported to have higher added value over their parent GCMs. Besides, added value of RCMs over GCMs was reported in some studies for mean temperature and Indian summer monsoon (ISM) simulations over the Himalayan region.[58,59] Jury et al.[59] reported added value in the downscaled simulations CORDEX-SA and CORDEX EA RCMS over their driving GCMs in terms of higher spatial correlation with the observation in temperature as compared to their driving GCMS in elevation-dependent warming in the Himalayan region. Simulation of climate impact indices shows that, while models perform better in reproducing percentile-based thresholds, they differ in terms of extreme threshold which should be considered when selecting the criteria of heat wave simulation.

Following the bias correction, heat wave events were simulated, and it was found that the models simulated heat wave in the regions of high frequency as in observation, i.e., northwestern, central, and south-central region. Mandal et al.[60] also reported high heat wave occurrences in the northwestern, central, and south-central region over India and declared northwestern and south-central region heat wave-prone regions of the country based on severity. Singh et al.[8] also reported the regions showing highest heat wave frequency in the country with significant increase in the last seven decades. The heat wave trend analysis shows that majority of the models are performing better in the northwestern and central Indian region followed by the western and south-central region, which records the highest heat wave events in the country, but fails to capture the decreasing trend in eastern region. The differences in the heat wave trend simulation among the ensemble members may be attributed to the lateral boundary condition application procedure and physical parameterization of the models. The uncertainty due to different downscaling RCMs can be seen in heat wave trend shown by CanESM2, CNRM-CM5, CSIRO-Mk3.6, and GFDL-ESM2M, where SMHI_ RCA4 downscaled RCMs show an overestimation showing HW occurrences in the region where no HW is recorded by IITM-RegCM4 downscaled RCMs. Similar trends in both magnitude and spatial variability over India are observed in case of MPI-ESM-LR downscaled by SMHI_RCA4 and MPI-CSC-REMO2009 with SMHI_MPI-ESM-LR showing some spatial overestimation in the eastern and south-central region. The failure of models in capturing the decreasing trend in the eastern region may be attributed to an overestimation of temperature in the eastern region owing to positive temperature bias over the Bay of Bengal region due to lack of moisture and dry bias in adjoining areas.[45,48,56] The overestimation of temperature leads to high frequency of heat waves in the eastern region of the country as compared to the observation and so the decline could not be captured. CSIRO-Mk3.6-simulated heat wave events were found to be closer to the observation from both the ensembles. The downscaled simulations of CSIRO- Mk3.6 in the CORDEX-SA experiment have also been reported to have higher added value over their parent GCMs. Choudhary et al.[38] reported the added value of RCMs in comparison to the GCMs in simulating ISM and found that RegCM4 downscaled model simulations simulated the ISM better than the parent GCM with the highest added value reported in the downscaled simulations of the GCM-CSIRO-Mk3-6-0. Considering the added value of the RCMs observed in simulating the ISM (precipitation) over the Himalayan region, temperature simulations which are affected by the wet bias would provide this added value in the RCMs. The findings support our study where the downscaled CSIRO-Mk3-6-0 (RCM) simulations were best among the historical simulations of maximum temperature and heat wave events. Future projection of heat waves was assessed using all RCM simulations to provide a high-resolution regional climate signal of changing characteristics of heat wave over India under RCP 4.5 and RCP 8.5 scenario emission trajectories and highlight the region which can possibly emerge as future heat wave hotspots. The projection

shows that heat waves will continue to increase over the northwestern, central, south-central region, and southern coastal region in both the scenarios. Heat wave events are found to be extended to the southern region of the country which was not observed in the historical period in both scenarios.

According to the assumptions of the RCP 4.5 scenario that suggests emissions to peak during mid-century and further decline in end of the century, a decrease in the spatial extent of occurrence of heat wave events is observed. But heat wave events show spatial strengthening over most of the country recording higher frequency in the eastern region of the country as well projecting an increase in magnitude of occurrence in the RCP 8.5 scenario. This increase is much more pronounced in the RCP 8.5 scenarios than RCP 4.5 scenarios due to increasing temperature as well as increasing area under high temperatures in the RCP 8.5 scenarios. For the long-term future period under RCP 8.5 scenarios, the spatial patterns clearly indicate the prevalence of heat extremes all over India as simulated by the majority of the models. The variations among the heat wave projections among the models reflect the uncertainty resulting from three different RCMs used for downscaling and so present different possible heat wave futures over India. Though the range of uncertainty between the ensembles is more, the spread of the uncertainty within the ensemble is considerably less in terms of both spatial and temporal frequencies. Among the regions reporting higher heat waves, the largest increase among the three heat wave-prone regions is projected for the south-central region in future. This increase in south-central region as projected by the models has also been reported by Dubey et al.[61] who found south-central region to observe high heat wave hazard in future scenarios using REMO-OASIS-MPIOM model over India. While increase in global temperature will escalate heat wave events over India, modulation in the characteristics phenomenon of natural climate variability, increasing sea surface temperature, strengthening of mid-tropospheric high, changing land-surface interactions due to changing land use and land cover, reduced soil moisture and increased sensible heat flux,[12] and erratic monsoon causing delay in monsoon or absence of pre-monsoon activity would further influence and exacerbate these rising trends.[11,18,22,43,46] The increase in frequency is higher as compared to duration and intensity and so there will be more frequent heat wave events which will pose extreme risk to health, agriculture, infrastructure, energy demands, and socio-economic issues and loss of productivity in India.

Conclusion

The study analyzes the future changes in the characteristics of heat wave events over India using 17 CORDEX-SA RCM simulations and their means. It was found that the models observed warm and cold bias in climatological mean simulation which was further removed by applying the variance scaling bias correction method. While variance scaling corrected model biases and improved the statistical distribution of the temperature, it was found that the models simulated fixed thresholds (TX95t) better than peak temperature (TXx). Heat wave characteristics simulation shows all RCMs to capture heat wave occurrence in the heat wave hotspots, i.e., Northern, Northwestern, Central, and South-Central India. Among all the RCMs IITM_CSIRO-Mk3.6 and IITM_GFDL-ESM2M, SMHI_CSIRO-Mk3.6, SMHI_IPSL-CM5A-MR, and SMHI_EC-EARTH capture frequency, intensity, and duration similar to observation making them more reliable models in future heat wave projections. The average range of heat wave future projections as simulated by the models showed that a four- to seven-fold increase in heat wave events is projected for mid-term and long-term future under RCP 4.5 scenario spatially for different regions, which may rise to five- to 10-fold under RCP 8.5 scenario. CSIRO-Mk3.6, the best model, shows the highest increase of 20 events/year to 35 events/year in mid-term and long-term period under RCP 4.5 scenario and 25 events/year to 60 events/year under RCP 8.5 scenario, whereas the best estimate obtained from an average of all the models indicates an overall median increase of 4 (mid-term) to 6 events (long-term) under RCP 4.5 scenario and 6 events (mid-term) to 20 events (long-term) from historical season under RCP 8.5 scenario for India. Northwestern, central, and south-central region of the country recorded the highest heat wave events in both the future scenarios with largest increase in the south-central region and so the region may become a future heat wave hotspot. Among the ensembles, it is found that SMHI ensemble member models project a higher increase in heat wave events as compared to IITM ensemble models and RE_MPI-ESM-LR simulate similar to IITM ensemble members. Heat wave events are found to become more intense in the future with maximum intensity reaching 54°C–59°C by the end of the century under RCP 8.5 scenario, and duration is projected to rise up to by 22 days–51 days under RCP 8.5 scenario. Importantly, the rise in frequency is much larger than the increase in intensity and so in future there would be higher number of heat wave events over India. Also, it brings to the attention the elevated risk to human health in the future. Along with the three heat wave hotspot regions which face health risk due to rising frequency of events, the coastal region of Odisha and Andhra Pradesh may be severely affected, where heat waves have been found to be significantly associated with mortality.[8] Any increase in heat wave will only aggravate the health risk causing deadly episodes of mortality over this heat-vulnerable region. With India becoming the largest population country, heat waves events may have disastrous consequences such as mass morbidity and mortality in future and also pose a challenge for fulfilling the sustainable development goals. The study concludes that an unquestionable multi-fold increase in frequency, intensity, and duration in heat wave events awaits over India which will exacerbate the health hazard, threaten food security, as well as decrease productivity thereby increasing economic burden. Thus, the study recommends a holistic heat-resilient future pathway through adopting adequate mitigation and adaptation strategies for India prioritizing the regional variations observed in the study for future emerging hotspots that need action at the earliest.

Limitations of the study

The study presents an overall scenario of future change in heat wave characteristics over India and identifies the regions of concerns (hotspots) in future for India. The findings would aid the policy makers in designing a robust heat preparedness plan for India. However, more insights could be gained by analyzing the impact of global circulations, land-atmospheric feedback, land use, and land cover change on changing

heat wave trends over India which were beyond the scope of present study. These are the potential areas of research on heat waves over India using RCM and so pave way for future heat wave research.

STAR★METHODS

Detailed methods are provided in the online version of this paper and include the following:

- KEY RESOURCES TABLE
- RESOURCE AVAILABILITY
  - Lead contact
  - Materials availability
  - Data and code availability
- METHOD DETAILS
  - Data
  - Bias correction
- QUANTIFICATION AND STATISTICAL ANALYSIS
  - Performance indicators
  - Climate impact indices
  - Heat wave criteria

SUPPLEMENTAL INFORMATION

Supplemental information can be found online at https://doi.org/10.1016/j.isci.2023.108263.

ACKNOWLEDGMENTS

Authors thank the Climate Change Program, Department of Science and Technology, New Delhi, for financial support (DST/CCP/CoE/80/2017(G)). Authors gratefully acknowledged the World Climate Research Program's Working Groups, former coordinating body of CORDEX and CMIP5. The climate modeling groups (listed in Table 1) are sincerely thanked for producing and making available their model output. The authors thank the Earth System Grid Federation (ESGF) infrastructure esgf data node for providing CORDEX South Asia data. Authors also gratefully acknowledge the climate data provided by the India Meteorological Department, New Delhi.

Funding information: Authors thank the Climate Change Program, Department of Science and Technology, New Delhi, for financial support (DST/CCP/CoE/80/2017(G)).

AUTHOR CONTRIBUTIONS

R.K.M., Supervision, Funding Acquisition, & Resources; R.K.M. and S.S., Conceptualization & Design; S.S., Investigation; R.K.M. and S.S., Writing, Reviewing & Editing. All authors read and approved the final manuscript.

DECLARATION OF INTERESTS

The authors declare no competing interests.

INCLUSION AND DIVERSITY

We support inclusive, diverse and equitable conduct of research.

Received: February 15, 2023
Revised: July 29, 2023
Accepted: October 17, 2023
Published: October 19, 2023

REFERENCES

1. IPCC. (2021). Summary for Policymakers. In Climate Change 2021: The Physical Science Basis. Contribution of Working Group I to the Sixth Assessment Report of the Intergovernmental Panel on Climate Change, V. Masson-Delmotte, P. Zhai, A. Pirani, S.L. Connors, C. Péan, Y. Chen, L. Goldfarb, M.I. Gomis, J.B.R. Matthews, and S. Berger, et al., eds. (Cambridge University Press), pp. 3–32. https://doi.org/10.1017/9781009157896.001.

2. Perkins-Kirkpatrick, S.E., and Gibson, P.B. (2017). Changes in regional heatwave characteristics as a function of increasing global temperature. Sci. Rep. *7*, 12256–12312.

3. Mall, R.K., Singh, R., Gupta, A., Srinivasan, G., and Rathore, L.S. (2006). Impact of climate change on Indian agriculture: A review. Clim. Change *78*, 445–478.

4. Anderson, G.B., and Bell, M.L. (2011). Heat waves in the United States: mortality risk during heat waves and effect modification by heat wave characteristics in 43 US communities. Environ. Health Perspect. *119*, 210–218.

5. Mazdiyasni, O., Aghakouchak, A., Davis, S.J., Madadgar, S., Mehran, A., Ragno, E., Sadegh, M., Sengupta, A., Ghosh, S., Dhanya, C.T., and Niknejad, M. (2017). Increasing

probability of mortality during Indian heat waves. Sci. Adv. *3*, e1700066–6.
6. Sonkar, G., Mall, R.K., Banerjee, T., Singh, N., Kumar, T.V.L., and Chand, R. (2019). Vulnerability of Indian wheat against rising temperature and aerosols. Environ. Pollut. *254*, 112946.
7. Singh, N., Singh, S., and Mall, R.K. (2020). Urban ecology and human health: implications of urban heat island, air pollution and climate change nexus. In Urban Ecology, P. Verma, P.A. Singh, R. Singh, and A.S. Raghubanshi, eds. (Elsevier), pp. 317–334.
8. Singh, S., Mall, R.K., and Singh, N. (2021). Changing spatio-temporal trends of heat wave and severe heat wave events over India: An emerging health hazard. Int. J. Climatol. *41*, E1831–E1845.
9. Kumar, P., Rai, A., Upadhyaya, A., and Chakraborty, A. (2022). Analysis of heat stress and heat wave in the four metropolitan cities of India in recent period. Sci. Total Environ. *818*, 151788.
10. Perkins, S.E. (2015). A review on the scientific understanding of heatwaves-Their measurement, driving mechanisms, and changes at the global scale. Atmos. Res. *164–165*, 242–267.
11. Ratnam, J.V., Behera, S.K., Ratna, S.B., Rajeevan, M., and Yamagata, T. (2016). Anatomy of Indian heatwaves. Sci. Rep. *6*, 24395–24411.
12. Ghatak, D., Zaitchik, B., Hain, C., and Anderson, M. (2017). The role of local heating in the 2015 Indian Heat Wave. Sci. Rep. *7*, 7707–7708.
13. Mall, R.K., Chaturvedi, M., Singh, N., Bhatla, R., Singh, R.S., Gupta, A., and Niyogi, D. (2021). Evidence of asymmetric change in diurnal temperature range in recent decades over different agro-climatic zones of India. Int. J. Climatol. *41*, 2597–2610. https://doi.org/10.1002/joc.6978.
14. Russo, S., Sillmann, J., and Fischer, E.M. (2015). Top ten European heatwaves since 1950 and their occur- rence in the future. Environ. Res. Lett. *10*, 124003.
15. Wang, L., Ranasinghe, R., Maskey, S., van Gelder, P.H.A.J.M., and Vrijling, J.K. (2016). Comparison of empirical statistical methods for downscaling daily climate projections from CMIP5 GCMs: A case study of the Huai River Basin, China. Int. J. Climatol. *36*, 145–164.
16. Rajput, P., Singh, S., Singh, T.B., and Mall, R.K. (2023). The nexus between climate change and public health: a global overview with perspectives for Indian cities. Arab. J. Geosci. *16*, 15.
17. Pai, D.S., Nair, S., and Ramanathan, A.N. (2013). Long term climatology and trends of heat waves over India during the recent 50 years (1961-2010). Mausam *64*, 585–604.
18. Rohini, P., Rajeevan, M., and Srivastava, A.K. (2016). On the Variability and Increasing Trends of Heat Waves over India. Sci. Rep. *6*, 26153–26159.
19. Zachariah, M.T.A., AchutaRao, K., Saeed, F., Jha, R., Dhasmana, M.K., and Mondal, A. (2022). Climate Change made devastating early heat in India and Pakistan 30 times more likely (World Weather Attribution), p. 43. https://www.worldweatherattribution.org/climate-change-made-devastating-early-heat-in-india-and-pakistan-30-times-more-likely/.
20. Sillmann, J., Kharin, V.V., Zhang, X., Zwiers, F.W., and Bronaugh, D. (2013). Climate extremes indices in the CMIP5 multimodel ensemble: Part 1. Model evaluation in the present climate. J. Geophys. Res. Atmos. *118*, 1716–1733.
21. Sillmann, J., Kharin, V.V., Zwiers, F.W., Zhang, X., and Bronaugh, D. (2013). Climate extremes indices in the CMIP5 multimodel ensemble: Part 2. Future climate projections. JGR. Atmospheres *118*, 2473–2493.
22. Alexander, L.V., and Arblaster, J.M. (2017). Historical and projected trends in temperature and precipitation extremes in Australia in observations and CMIP5. Weather Clim. Extrem. *15*, 34–56.
23. Mall, R.K., Singh, N., Singh, K.K., Sonkar, G., and Gupta, A. (2018). Evaluating the performance of RegCM4.0 climate model for climate change impact assessment on wheat and rice crop in diverse agro-climatic zones of Uttar Pradesh, India. Clim. Change *149*, 503–515.
24. Kim, G., Cha, D.H., Park, C., Jin, C.S., Lee, D.K., Suh, M.S., Oh, S.G., Hong, S.Y., Ahn, J.B., Min, S.K., and Kang, H.S. (2020). Evaluation and Projection of Regional Climate over East Asia in CORDEX-East Asia Phase I Experiment. Asia. Pac. J. Atmos. Sci. *57*, 119–134.
25. Meehl, G.A., Covey, C., Delworth, T., Latif, M., McAvaney, B., Mitchell, J.F.B., Stouffer, R.J., and Taylor, K.E. (2007). The WCRP CMIP3 multimodel dataset: A new era in climatic change research. Bull. Am. Meteorol. Soc. *88*, 1383–1394.
26. Giorgi, F., Jones, C., and Asrar, G. (2009). Addressing climate information needs at the regional level: the CORDEX framework (WMO), pp. 175–183.
27. Rajczak, J., and Schär, C. (2017). Projections of Future Precipitation Extremes Over Europe: A Multimodel Assessment of Climate Simulations. JGR. Atmospheres *122*, 773–810.
28. Singh, S., Mall, R.K., Dadich, J., Verma, S., Singh, J.V., and Gupta, A. (2021). Evaluation of CORDEX- South Asia regional climate models for heat wave simulations over India. Atmos *248*, 105228.
29. Tang, J., Niu, X., Wang, S., Gao, H., Wang, X., and Wu, J. (2016). Statistical downscaling and dynamical downscaling of regional climate in China: Present climate evaluations and future climate projections. JGR. Atmospheres *121*, 2110–2129.
30. Gutowski Jr, W.J., Giorgi, F., Timbal, B., Frigon, A., Jacob, D., Kang, H.S., Raghavan, K., Lee, B., Lennard, C., Nikulin, G., et al. (2016). WCRP Coordinated Regional Downscaling Experiment (CORDEX): A diagnostic MIP for CMIP6. Geosci. Model Dev. *9*, 4087–4095.
31. Giorgi, F. (2019). Thirty Years of Regional Climate Modeling : Where Are We and Where Are We Going next. JGR. Atmospheres *124*, 5696–5723.
32. Plavcová, E., and Kyselý, J. (2012). Atmospheric circulation in regional climate models over Central Europe: Links to surface air temperature and the influence of driving data. Clim. Past *Dyn39*, 1681–1695.
33. Kotlarski, S., Keuler, K., Christensen, O.B., Colette, A., Déqué, M., Gobiet, A., Goergen, K., Jacob, D., Lüthi, D., van Meijgaard, E., et al. (2014). Regional climate modeling on European scales: A joint standard evaluation of the EURO-CORDEX RCM ensemble. Geosci. Model Dev. *7*, 1297–1333.
34. Xu, Z., Han, Y., and Yang, Z. (2019). Dynamical downscaling of regional climate : A review of methods and limitations. Sci. China Earth Sci. *62*, 365–375.
35. Seneviratne, S.I., and Hauser, M. (2020). Regional Climate Sensitivity of Climate Extremes in CMIP6 Versus CMIP5 Multimodel Ensembles. Earth's Future *8*, e2019EF001474–17.
36. Mukherjee, S., and Mishra, V. (2018). Concurrent day and nighttime heatwaves in India under 1.5, 2.0, and 3.0°C warming worlds. Sci. Rep. *8*, 16922.
37. Choudhary, A., Dimri, A.P., and Maharana, P. (2018). Assessment of CORDEX-SA experiments in representing precipitation climatology of summer monsoon over India. Theor. Appl. Climatol. *134*, 283–307.
38. Choudhary, A., Dimri, A.P., and Paeth, H. (2019). Added value of CORDEX-SA experiments in simulating summer monsoon precipitation over India. Int. J. Climatol. *39*, 2156–2172.
39. Li, D., Yin, B., Feng, J., Dosio, A., Geyer, B., Qi, J., Shi, H., and Xu, Z. (2018). Present climate evaluation and added value analysis of dynamically downscaled simulations of CORDEX-East Asia. J. Appl. Meteorol. *57*, 2317–2341.
40. Molina, M.O., Sánchez, E., and Gutiérrez, C. (2020). Future heat waves over the Mediterranean from an Euro- CORDEX regional climate model ensemble. Sci. Rep. *10*, 8801.
41. Sanjay, J., Krishnan, R., Shrestha, A.B., Rajbhandari, R., and Ren, G.Y. (2017). ScienceDirect Downscaled climate change projections for the Hindu Kush Himalayan region using CORDEX South Asia regional climate models. Adv. Clim. Chang. Res. *8*, 185–198.
42. Prajapat, D.K., Lodha, J., and Choudhary, M. (2020). spatiotemporal analysis of Indian warming target using CORDEX-SA experiment data. Theor. Appl. Climatol. *139*, 447–459.
43. Murari, K.K., Ghosh, S., Patwardhan, A., Daly, E., and Salvi, K. (2015). Intensification of future severe heat waves in India and their effect on heat stress and mortality. Reg. Environ. Change *15*, 569–579.
44. Das, J., and Umamahesh, N.V. (2021). Heat Wave Magnitude over India under Changing Climate: Projections fromCMIP5 and CMIP6 Experiments. Int. J. Climatol. *42*, 331–351.
45. Mishra, V., Mukherjee, S., Kumar, R., and Stone, D.A. (2017). Heat wave exposure in India in current, 1.5°C, and 2.0°C worlds. Environ. Res. Lett. *12*, 124012.
46. Rohini, P., Rajeevan, M., and Mukhopadhay, P. (2019). Future projections of heat waves over India from CMIP5 models. Clim. Dyn. *53*, 975–988.
47. Dubey, A.K., and Kumar, P. (2022). Future projections of heatwave characteristics and dynamics over India using a high-resolution regional earth system model. Clim. Dyn. *60*, 127–145.
48. Rai, P., Choudhary, A., and Dimri, A.P. (2020). Future precipitation extremes over India from the CORDEX-South Asia experiments. Theor. Appl. Climatol. *137*, 2961–2975.
49. Panday, P.K., Thibeault, J., and Frey, K.E. (2015). Changing temperature and precipitation extremes in the Hindu Kush-Himalayan region: an analysis of CMIP3 and CMIP5 simulations and projections. Int. J. Climatol. *35*, 3058–3077.
50. Mishra, S.K., Sahany, S., Salunke, P., Kang, I.-S., and Jain, S. (2018). Fidelity of CMIP5

multi-model mean in assessing Indian monsoon simulations. npj Clim. Atmos1 *1*, 39.
51. Dimri, A.P., Kumar, D., Choudhary, A., and Maharana, P. (2018). Future changes over the Himalayas: mean temperature. Glob. Planet *162*, 235–251.
52. Dimri, A.P., Kumar, D., Choudhary, A., and Maharana, P. (2018). Future changes over the Himalayas: maximum and minimum temperature. Glob. Planet *162*, 212–234.
53. Nayak, S., Mandal, M., and Maity, S. (2019). Performance evaluation of RegCM4 in simulating temperature and precipitation climatology over India. Theor. Appl. Climatol. *137*, 1059–1075.
54. Nengker, T., Choudhary, A., and Dimri, A.P. (2017). Assessment of the performance of CORDEX-SA experiments in simulating seasonal mean temperature over the Himalayan region for the present climate: part I. Clim. Dyn. *50*, 2411–2441.
55. Kumar, P., Sarthi, P.P., Kumar, S., Barat, A., and Sinha, A.K. (2020). Evaluation of CORDEX-RCMS and their driving GCMs of CMIP5 in simulation of Indian summer monsoon rainfall and its future projections. Arab. J. Geosci. *13*, 225.
56. Kumar, P., Mishra, A.K., Dubey, A.K., Javed, A., Saharwardi, M.S., Kumari, A., Sachan, D., Cabos, W., Jacob, D., and Sein, D.V. (2022). Regional earth system modelling framework for CORDEX-SA: an integrated model assessment for Indian summer monsoon rainfall. Clim. Dyn. *59*, 2409–2428.
57. Choudhary, A., and Dimri, A.P. (2019). Performance of an ensemble of CORDEX-SA simulations in representing maximum and minimum temperature over the Himalayan region. Theor. Appl. Climatol. *136*, 1047–1072.
58. Haslinger, K., Anders, I., and Hofstätter, M. (2013). Regional climate modelling over complex terrain: an evaluation study of COSMO- CLM hindcast model runs for the Greater Alpine Region. Clim. Dyn. *40*, 511–529.
59. Jury, M.W., Mendlik, T., Tani, S., Truhetz, H., Maraun, D., Immerzeel, W.W., and Lutz, A.F. (2020). Climate projections for glacier change modelling over the Himalayas. Int. J. Climatol. *40*, 1738–1754.
60. Mandal, R., Joseph, S., Sahai, A.K., Phani, R., Dey, A., Chattopadhyay, R., and Pattanaik, D.R. (2019). Real time extended range prediction of heat waves over India. Sci. Rep. *9*, 9008.
61. Dubey, A.K., Lal, P., Kumar, P., Kumar, A., and Dvornikov, A.Y. (2021). Pre- sent and future projections of heatwave hazard-risk over India: a regional earth system model assessment. Environ. Res. *201*, 111573.
62. Srivastava, A.K., Rajeevan, M., and Kshirsagar, S.R. (2009). Development of a high-resolution daily gridded temperature data set (1969–2005) for the Indian region. Atmos. Sci. Lett. *10*, 249–254.
63. Christensen, J.H., Boberg, F., Christensen, O.B., and Lucas-Picher, P. (2008). On the need for bias correction of regional climate change projections of temperature and precipitation. Geophys. Res. Lett. *35*, L20709.
64. Chen, J., Brissette, F.P., Chaumont, D., and Braun, M. (2013). Finding appropriate bias correction methods in downscaling precipitation for hydrologic impact studies over North America. Water Resour. Res. *49*, 4187–4205.
65. Themeßl, M.J., Gobiet, A., and Heinrich, G. (2012). Empirical-statistical downscaling and error correction of regional climate models and its impact on the climate change signal. Clim. Change *112*, 449–468.
66. Teutschbein, C., and Seibert, J. (2012). Bias correction of regional climate model simulations for hydrological climate-change impact studies: Review and evaluation of different methods. J. Hydrol *456–457*, 12–29.
67. Bhatla, R., Sarkar, D., Verma, S., Sinha, P., Ghosh, S., and Mall, R.K. (2020). Regional climate model performance and application of bias corrections in simulating summer monsoon maximum temperature for agro-climatic zones in India. Theor. Appl. Climatol. *142*, 1595–1612.
68. Taylor, K.E. (2001). Sumarizing multiple aspects of model performance in a Single Diagram. J. Geophys. Res. *106*, 7183–7192.
69. Perkins, S.E. (2011). Biases and model agreement in projections of climate extremes over the tropical Pacific. Earth Interact. *15*, 1–36.
70. O'Brien, T.A., Kashinath, K., Cavanaugh, N.R., Collins, W.D., and O'Brien, J.P. (2016). A fast and objective multidimensional kernel density estimation method: FastKDE. Comput. Stat. Data Anal. *101*, 148–160.

STAR★METHODS

KEY RESOURCES TABLE

REAGENT or RESOURCE	SOURCE	IDENTIFIER
Software and algorithms		
CORDEX -SA regional climate model dataset	Coupled Model Intercomparison Project	CORDEX-SA database: https://esgf-data.dkrz.de/search/esgf-dkrz/
Observed maximum temperature data	India Meteorological Department	IMD database: https://cdsp.imdpune.gov.in/ https://github.com/sam0a/Heat_wave_iscience.git
R 4.1.2	The Comprehensive R Archive Network	https://cran.r-project.org/
MATLAB 2019b	Mathworks	https://in.mathworks.com/

RESOURCE AVAILABILITY

Lead contact

Further information and requests for resources should be directed to and will be fulfilled by the lead contact, R. K. Mall (rkmall@bhu.ac.in).

Materials availability

This study did not generate new unique reagents.

Data and code availability

- The study analyses existing, publicly available data. All of the CORDEX -SA regional climate model data used in the study is archived at Earth System Grid Federation data node and is publicly available at https://esgf-data.dkrz.de/search/esgf-dkrz/.
- The IMD data can be accessed on upon request from https://cdsp.imdpune.gov.in/ and is provided at the repository with the links listed in the key resources table. All original code has been deposited at GitHub and is publicly available as of the date of publication on https://github.com/sam0a/Heat_wave_iscience.git.
- Any additional information required to reanalyze the data reported in this paper is available from the lead contact upon request.

METHOD DETAILS

Data

The study aims to evaluate model performance for historical period (1971–2005) and assess the changes in heat wave events over India for mid-term (2041–2060) and long-term future (2081–2099) period under RCP 4.5 and RCP 8.5 scenarios during March-June when heat waves are most observed over India. The study area extends over the Indian region 8°4′ N to 37°6′ N latitude and 68° 7′ E to 97°25′ E longitude in CORDEX–SA domain of 19°15′ E to 116° 15′ E and 15° 45′ S to 45° 45′ N, as shown in below figure. Daily gridded observed maximum temperature data developed by Srivastava et al.[62] at a resolution of 50 km is obtained from India Meteorological Department (IMD) for the historical period 1971–2005 (March-June).

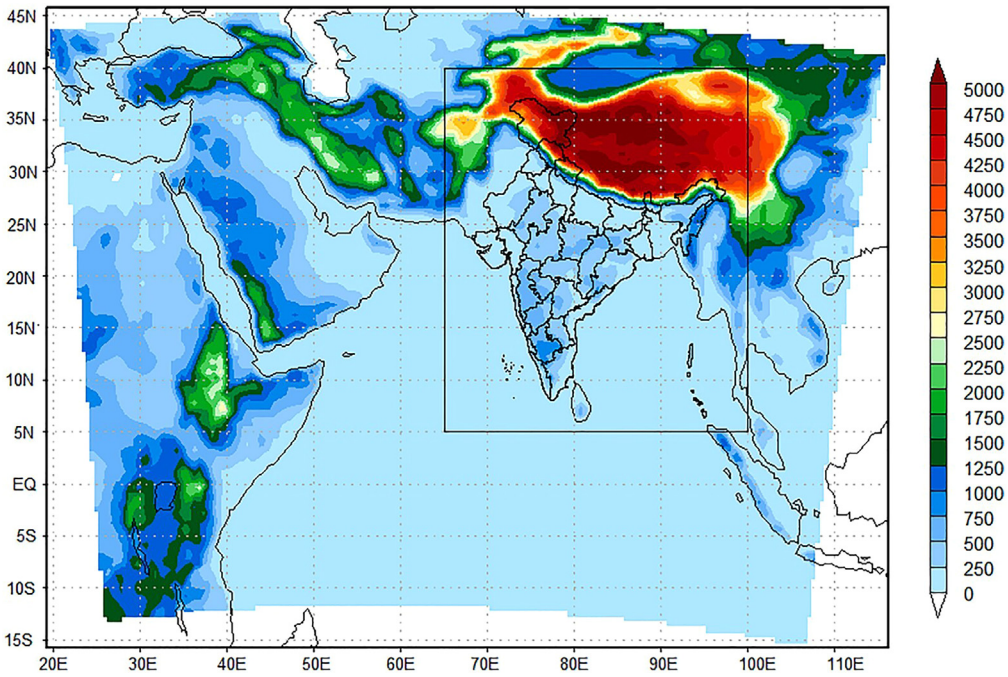

Map showing topography (in meters) of the Indian region highlighted by the rectangular box within the CORDEX-SA domain extending over 19° 15′ E to 116° 15′ E and 15° 45′ S to 45° 45′ N.

The study uses seventeen dynamically downscaled high resolution maximum temperature projections derived from ten coarse resolution Atmosphere-Ocean coupled General Circulation Models (AOGCMs) using three different RCMs (IITM-RegCM4, SMHI-RCA4, MPI-CSC-REMO2009) at 50 km spatial resolution from CORDEX SA experiment.[41] The specification of the CORDEX-SA experiments used in the study are given in below table. The RCM outputs are obtained from contributing climate modeling groups archived at Earth System Grid Federation data node (https://esgf-data.dkrz.de/search/esgf-dkrz/). In the paper, the RCM simulations will be referred by the name of the RCM followed by the GCM for e.g., SMHI_CanESM2. Among all the RCM simulations a consistent data for SMHI_EC-EARTH was not available for long-term future under both RCP 4.5 and RCP 8.5 scenario and for SMHI_CanESM2 for long term future under RCP 8.5 scenarios.

Details of CORDEX-SA RCMs used in the study

CORDEX South Asia RCM	RCM Description	Contributing CORDEX Modeling Center	Driving CMIP5 AOGCM (see details at https://verc.enes.org/data/enes-model-data/cmip5/resolution)	Contributing CMIP5 Modeling Center
IITM-RegCM4 (6 ensemble members)	The Abdus Salam International Centre for Theoretical Physics (ICTP) Regional Climatic Model version 4.4.5	Centre for Climate Change Research (CCCR), Indian Institute of Tropical Meteorology (IITM), India	CanESM2	Canadian Centre for Climate Modelling and Analysis (CCCma), Canada
			GFDL-ESM2M	National Oceanic and Atmospheric Administration (NOAA), Geophysical Fluid Dynamics Laboratory (GFDL), USA
			CNRM-CM5	Centre National de Recherches Météorologiques (CNRM), France
			MPI-ESM-MR	Max Planck Institute for Meteorology (MPI-M), Germany
			IPSL-CM5A-LR	Institut Pierre-Simon Laplace (IPSL), France
			CSIRO-Mk3.6	Commonwealth Scientific and Industrial Research Organization (CSIRO), Australia

(*Continued on next page*)

Continued

CORDEX South Asia RCM	RCM Description	Contributing CORDEX Modeling Center	Driving CMIP5 AOGCM (see details at https://verc.enes.org/data/enes-model-data/cmip5/resolution)	Contributing CMIP5 Modeling Center
SMHI-RCA4 (10 ensemble members)	Rossby Centre regional atmospheric model version 4	Rosssy Centre, Swedish Meteorological and Hydrological Institute (SMHI), Sweden	EC-EARTH	Irish Centre for High-End Computing (ICHEC), European Consortium (EC)
			MIROC5	Model for Interdisciplinary Research On Climate (MIROC), Japan Agency for Marine-Earth Sci. & Tech., Japan
			NorESM1-M	Norwegian Climate Centre (NCC), Norway
			HadGEM2-ES	Met Office Hadley Centre for Climate Change (MOHC), United Kingdom
			CanESM2	CCCma, Canada
			GFDL-ESM2M	NOAA, GFDL, USA
			CNRM-CM5	CNRM, France
			MPI-ESM-LR	MPI-M, Germany
			IPSL-CM5A-MR	IPSL, France
			CSIRO-Mk3.6	CSIRO, Australia
MPI-CSC-REMO2009	MPI Regional model 2009	Climate Service Center (CSC), Germany	MPI-ESM-LR	MPI-M, Germany

Bias correction

Bias correction of climate model data reduces the uncertainty associated with climate projections due to systemic error or model physical parameterization.[36,63,64] Understanding and removing the bias involves correction of statistical characteristics of the model data such as mean, variance, standard deviations, data distributions etc. Based on these principals, studies have used different approaches such as linear scaling, variance scaling, distribution mapping and delta change method to remove the bias associated with model simulations.[64,65] As individual RCM simulations have inherent biases, application of large ensemble RCM with bias correction is recommended to reduce the uncertainty in projections due to these biases.[27,66] Bias correction methods work on deriving a correction factor based on difference between model and observed data in the historical period and are stationary assuming that the correction factor remains valid for both present and future condition.[66]As there is no future reference/observation data present for validation of bias corrected data, researchers rely on the ability of methods to correct historical model data with respect to the observation for their application in future model data bias correction. Variance scaling has been widely used for bias correction of temperature data as it corrects both the mean and variance and produces same mean and variance after bias correction, narrowing the range of variability between observed and model data.[28,67,68] Teutschbein and Seibert,[66] reviewed and evaluated simple to sophisticated widely employed bias correction method and found that both variance scaling and distribution mapping methods perform better in fitting the mean and day to day variations in model simulated temperature data, and distribution mapping performed best for precipitation time series. In the present study, both historical and future i.e., 38 RCM simulations were bias corrected using variance scaling method (Equations 1–3).

$$T^{*2}_{contr}(d) = T^{*1}_{contr}(d) - \mu_m\left(T^{*1}_{contr}(d)\right) \quad \text{(Equation 1)}$$

$$T^{*3}_{contr}(d) = T^{*2}_{contr}(d) - \left[\frac{\sigma_m(T_{obs}(d))}{\sigma_m\left(T^{*2}_{contr}(d)\right)}\right] \quad \text{(Equation 2)}$$

$$T^{*}_{contr}(d) = T^{*3}_{contr}(d) + \mu_m\left(T^{*1}_{contr}(d)\right) \quad \text{(Equation 3)}$$

where $_{contr}$ is RCM-simulated 1971–2000, d is daily, $_{obs}$ is observed maximum temperature, σ is standard deviation, μ is mean, * is final bias corrected *1,2,3 is intermediated bias corrected model. A detailed explanation of the method can be found in Singh et al.[28]

QUANTIFICATION AND STATISTICAL ANALYSIS

Performance indicators

CORDEX-SA RCMs model performance is evaluated for simulating the observed climatological state such as the climatological mean maximum temperature, interannual variability, and extremes using a number of climatological and statistical metrics before and after bias correction (see table below). To measure the degree of overestimation and underestimation of RCM simulated mean maximum temperature, climatological mean (MEA-T) and mean bias (MB) is estimated over India.[33]The study uses standard performance metrics i.e., root-mean-square error (RMSE) and mean absolute error (MAE) to measure relative errors between model and observed, P_{BIAS} to estimate the percentage of bias, Wilmot's index of agreement (d) for determining the degree of agreement between model and observation and Taylor diagram to estimate the improvement in model simulated temperature dataset after bias correction[28,29,68] (see table below).

Model performance metrics and ET-SCI indices used in the study

Acronym	Metrics/Indices Name	Definition	Formula	Unit
MEA-T	Climatological mean	Climatological mean of maximum temperature	$\overline{X} = \frac{\sum_{i=1}^{n} X_i}{N}$	°C
MB	Mean Bias	Difference between model simulated and observed mean maximum temperature	$\frac{1}{n}\sum_{i=1}^{n}(M - O)$	°C
TXx	Max TX	Seasonal maximum value of daily maximum temperature	$TX_i = (\max)TX_i$	°C
TX95t	Very warm day threshold	Value of 95th percentile of TX	$TX95t = (0.95)TX_k$	T
RMSE	Root mean square error	square root of the mean of the square of all of the error	$\sqrt{\frac{\sum_{1}^{n}(M - O)^2}{n}}$	°C
MAE	Mean Absolute Error	arithmetic average of the absolute values of the differences between the members of each pair of observation and predicted values	$\frac{1}{n}\sqrt{\lvert M - O\rvert}$	°C
P_{BIAS}	Percent Bias	the percentage difference between the simulations from model and observation where positive values indicate overestimation and negative values indicate underestimation	$P_{Bias} = \frac{\sum_{i=1}^{n}(O_i - M_i)}{\sum_{i=1}^{n}(O_i)}$	%
D	Willmott's Index of Agreement	The ratio of the mean square error and the potential error (pe) multiplied by *n* (number of observations) and then subtracted from 1.	$d = 1 - \frac{\sum_{i=1}^{n}(O_i - M_i)^2}{\sum_{i=1}^{n}(\lvert M_i - \overline{O}\rvert + \lvert O_i - \overline{O}\rvert)^2}$	-
R^2	Correlation Coefficient	determines the strength of linear relationship between two variables. It lies between −1 and +1; *r* value equal to +1 indicates perfect and positive correlation, whereas negative value of −1 shows negative and perfect correlation.	$r = \frac{\sum_{=1}^{n}(O_i - \overline{O})(M_i - \overline{M})}{\sqrt{\sum_{i=1}^{n}(O_i - \overline{O})^2}\sqrt{\sum_{i=1}^{n}(M_i - \overline{M})^2}}$	°C

M denotes RCM output, O refers to the observed data and k is the number of values in the data.

Since, variance scaling approach produces same long-term mean value after bias correction, we evaluate the model performance and inter-ensemble variations in simulation of daily maximum temperature data before and after bias correction in comparison to the observation using standard multivariate probability distribution metrics.[69] In the study we use Kernel Density Estimation (KDE) and Empirical Cumulative Distribution Function (ECDF), the two probability density distributions for assessing model performance in simulating daily maximum temperature and capturing intra-annual variability for the historical period Mar-Jun (1971–2005). KDE is a non-parametric robust measure that gives the empirical estimate of probability density function irrespective of underlying distribution pattern assumption.[28,70] Similarly, ECDF is fitted to both daily model and observed temperature datasets to assess the probabilities of daily temperature values estimated before and after bias correction.[15]

Climate impact indices

Apart from these statistical measures, recently developed Expert Team on Sector-Specific Climate Indices (ET-SCI) which have a critical focus on sector specific responses have been used. In the present study two of the ET-SCI indices i.e., Seasonal maximum value of daily maximum temperature (TXx) and the 95th percentile of the seasonal maximum temperature referred to as Very Warm Day Threshold (TX95t) that measures impact on health, agriculture and economy are used for model performance evaluation. The intermodel spread in simulating the Tx95t

and TXx by the model simulations against observed provides a metric to assess the ability of RCMs in simulating extreme temperature over India (see table in performance indicators).

Heat wave criteria

Heat wave events are identified according the criteria given by IMD. The criteria is based on daily departure of maximum temperature from climatological normal where the reference period for climatological normal is 1970–2000. According to this criteria heat wave is declared if the maximum temperature of a station reaches at least $\geq 40^{\circ}$C for Plains, $\geq 37^{\circ}$C for coastal and at least $\geq 30^{\circ}$C for Hilly regions. Following criteria are used to declare heat wave.

i) Heat Wave: when the departure from normal temperature is 4.5°C–6.4°C

or

ii) Heat Wave: When the actual maximum temperature $\geq 45^{\circ}$C (for plains only)

To declare HW the above criteria should be met in at least two stations in a Meteorological sub-division for at least two consecutive days and the HW will be declared on the second day.

The impact of any heat wave event is a function of the three characteristic i.e., frequency, intensity and duration of the event.[2] Hence, it is essential to study and evaluate the model performance in reproducing the frequency, intensity and duration of heat wave events over India. In the present study, the frequency of the heat wave events is estimated as the number of heat wave events occurring during each season, intensity is the highest maximum temperature recorded during any event in the season and duration is the number of days in the longest heat wave event observed during the season for each grid.

To determine any possible long-term increasing or decreasing trend in the occurrence of heat waves, linear trends are estimated. Due to small sample size in the historical period, Student's *t* test at a confidence interval of 90% is used to test the robustness of the heat wave trends simulated by RCM ensemble models against observed.[28,46] Future changes in heat wave simulations are determined by difference between heat waves for near (2041–2069) and far future (2071–2099) period from the baseline period of 1971–2000.